European Journal of Medicinal Chemistry 207 (2020) 112723

Contents lists available at ScienceDirect

European Journal of Medicinal Chemistry

journal homepage: http://www.elsevier.com/locate/ejmech

Research paper

Nonpeptidic quinazolinone derivatives as dual nucleotide-binding oligomerization domain-like receptor 1/2 antagonists for adjuvant cancer chemotherapy

Yao Ma [a, 1], Jingshu Yang [b, 1], Xiduan Wei [b, 1], Yameng Pei [b], Jingjia Ye [b], Xueyuan Li [b], Guangxu Si [b], Jingyuan Tian [b], Yi Dong [a, **], Gang Liu [b, *]

[a] Institute of Materia Medica, Chinese Academy of Medical Sciences & Peking Union Medical College, 2A Nanwei Rd, Xicheng Dist, Beijing, 100050, PR China
[b] School of Pharmaceutical Sciences, Tsinghua University, Haidian Dist, Beijing, 100084, PR China

ARTICLE INFO

Article history:
Received 5 May 2020
Received in revised form
31 July 2020
Accepted 2 August 2020
Available online 14 August 2020

Keywords:
Quinazolinone
Dual NOD1/2 antagonists
Retroamide
B16 tumor

ABSTRACT

Nucleotide-binding oligomerization domain-containing protein 1 and 2 (NOD1/2) receptors are potential immune checkpoints. In this article, a quinazolinone derivative (**36b**) as a NOD1/2 dual antagonist was identified that significantly sensitizes B16 tumor-bearing mice to paclitaxel treatment by inhibiting both nuclear factor κB (NF-κB) and mitogen-activated protein kinase inflammatory signaling that mediated by NOD1/2.

1. Introduction

Currently, immunotherapy primarily aims to artificially stimulate the immune system to improve its natural ability to stop or eliminate cancer [1]. Therefore, the identification and evaluation of novel immune targets has become an important goal of research. Because the cytosolic nucleotide-binding oligomerization domain-containing protein 1 and 2 (NOD1 and NOD2) receptors are important components of the innate immune system, they have been pharmacologically targeted to enhance the immune response against cancer cells [2–7]. Many NOD1/2 agonists have been discovered: Mifamurtide, for example, has already been approved for treating high-grade, nonmetastatic, resectable osteosarcoma after surgical excision in children to young adults [8]. However, a shift has occurred in recent with the emerging knowledge that NOD antagonists facilitate the chemotherapy of some cancers [9]. For instance, Zitvogel and coworkers have identified the NOD2 receptor as a 'gut immune checkpoint' based on the evidence that NOD2 curtails cyclophosphamide (CTX)-induced cancer immunosurveillance by limiting the relocation of microbes [10]. Ferri's group demonstrated the NOD1 receptor as a putative therapeutic target in inflammation-mediated colon cancer metastasis. The experimental results revealed that NOD1 activation increased colorectal cancer cell adhesion, migration and metastasis via the p38 mitogen activated protein kinase pathway [11].

In 2011, we first reported a conjugate of paclitaxel (MTC-220, **1**) and a muramyl dipeptide (MDP) derivative that was superior to PTX alone for treatment of Lewis lung carcinoma (LLC) in mice. MDP is the natural ligand for NOD2, however, we found that the prototype for MTC-220 (compound **2**) is responsible for remodeling the tumor microenvironment (TME) by inhibiting NOD2 signaling and limiting PTX-induced cancer immunosurveillance in mice [12,13]. In addition, conjugates (**3** and **4**) of docetaxel (DTX) and MDP derivatives were designed as another chemical class of NOD1 antagonists for breast cancer treatment [14]. Effective antagonists for cancer adjuvant treatment should therefore antagonize both NOD1 and NOD2 signaling. Pharmacologically targeting both the NOD1 and NOD2 signaling pathways is expected to have a broad therapeutic utility for cancer treatment. Small molecules quinazolinones (**5**) and 2-aminobenzimidazoles (**6**) were discovered and identified

* Corresponding author.
** Corresponding author.
E-mail addresses: dongyi@imm.ac.cn (Y. Dong), gangliu27@tsinghua.edu.cn (G. Liu).
[1] These authors contributed equally.

https://doi.org/10.1016/j.ejmech.2020.112723
0223-5234/

as NOD1 antagonists in 2011 and 2014, respectively [15–17]. The NOD2 selective antagonist (**7**) is an imidazole derivative that was disclosed via high-throughput screening [18]. Jakopin's group reported in 2016 a dual NOD1/2 antagonist (Fig. 1, **8**) based on an indole scaffold [19,20]. Compound **9** was the first dual NOD1/2 antagonist based on a 1,4-benzodiazepine-2,5-dione derivative which sensitized chemotherapy with PTX to LLC in animals [21]. In this article, we perform the synthesis and evaluation of quinazolinone derivatives aiming to identify novel NOD1/2 dual antagonists. We have demonstrated compound **36b** as a novel NOD1/2 dual antagonist that can significantly sensitize B16 tumor-bearing mice to PTX treatment.

2. Results and discussion

2.1. The discovery of quinazolinone analogues 14 via screening

Initially, we performed a screening of a small quinazolinone library (approximately 50 compounds) that was previously established by our group aiming to identify novel NOD1/2 antagonists [22]. The library included fused-quinazolinone compounds (**10**, **11**), spiro-quinazolinone compounds (**12**) and other structurally diverse quinazolinones with different substitutions at the C2 position (**13**–**15**) (Fig. 2). All the compounds were tested at a concentration of 5 μM. The results revealed that compounds **10**–**13** and **15** exhibited relatively weak antagonistic percentage of NOD1/2 by either C12-iE-DAP or MDP stimulation with less than 50% inhibition. However, quinazolinones bearing free substitution at the C2 position (**14a, 14b**) displayed interesting antagonistic activities with their IC_{50} (NOD1/2) of 1.15/0.99 μM and IC_{50} (NOD1/2) of ND/0.8 μM), respectively, to both NOD1/2 by C12-iE-DAP or MDP stimulated HEK-Blue hNOD1/2 cells. Subsequently, the compounds of 3,6,7-substituents (R^3, R^5, R^4) of **14** are considered for further structure-activity relationship (SAR) and structure-metabolism relationship (SMR) investigation (Fig. 2).

2.2. Chemistry

The synthetic route to the quinazolinones in Tables 1–3 is illustrated in Scheme 1. 3-Chlorobenzoic acid (**16**) underwent a nitration by treating with KNO_3 and concentrated H_2SO_4 to give intermediate **17,** which further reacted with phenol derivatives to afford the intermediates (**18a-18e**), followed by amidation to prepare the corresponding amides (**19a-19g**). The nitro group of **19** was then reduced in the presence of Fe powder and formic acid, and the cyclization intermediates (**20a-20g**) were gained in one-pot. Removal of the formyl group by treating with a concentrated HCl gave the intermediates **21a-21g**, which underwent amidation to give the **14a-14b** and **22a**-**22t**. Intermediates of **23a** and **23b** were attained after hydrolysis of **14a** and **22n**, and subsequent amidation of **23a** and **23b** gave the desired **24a-24e**.

The synthesis of the retroamide quinazolinone analogues is illustrated in Scheme 2. Commercially available dimethyl 2-aminoterephthalate (**25**) underwent an iodination to give the intermediate **26** that further reacted with phenylboronic acid derivatives via Suzuki coupling to afford the biphenyl intermediates **27a**-**27c**. Subsequent hydrolysis yielded the corresponding acids **28a-28c**. Treatment with formamide resulted in the quinazolinone intermediates **29a-29c**, which were subsequently transformed into the desired compounds **30a-30j** through amidation with a variety of amine analogues. Compounds **28a-28c** reacted with triphosgene to afford cyclic intermediates **31a-31b** that underwent amidation by treating with methyl glycinate hydrochloride to give the intermediates **32a-32b**. Cyclization and amidation provided the compounds **34a-34f**, and **34f** was hydrolyzed to afford the acid **35**. Subsequent amidation gave the final analogues **36a-36b**.

2.3. Structure-activity relationship (SAR) and structure-metabolism relationship (SMR) studies

In R^4, removal of 4-CF_3 (**22a**) of 4-CF_3-benzyloxy ether or replacement of 4-CF_3 with 4-CN (**22b**), 4-F (**22c**) or 4-Cl (**22d**) of **14a** led to a decrease in activity, which indicates that 4-CF_3 is necessary

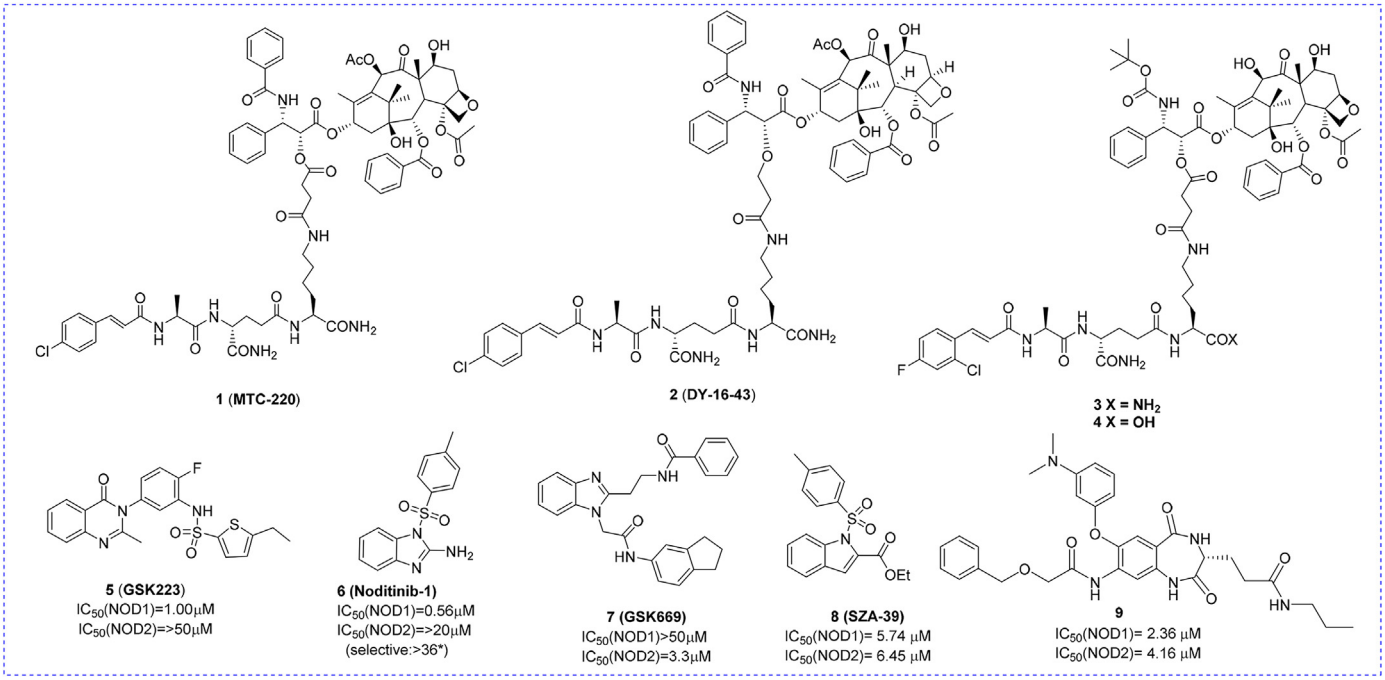

Fig. 1. Representative reported NOD1/2 antagonists.

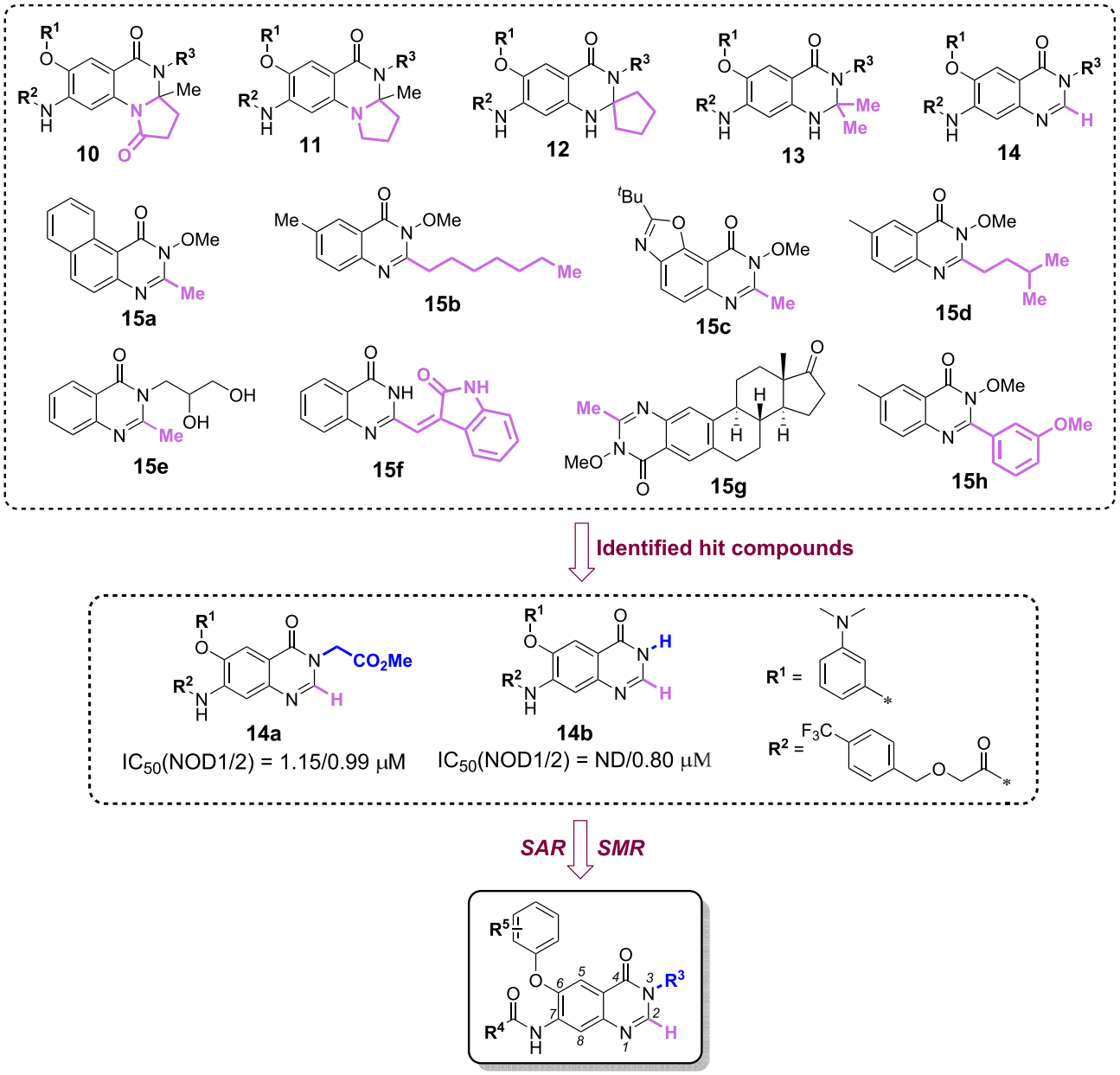

Fig. 2. Identification of hit compounds **14a** and **14b** via screening of quinazolinone derivatives.

for NOD 1/2 signaling antagonistic activity (Table 1). Acceptable NOD1 inhibitory percentage (70.88%) was observed by **22e** in which the 4-CF_3-benzyloxy ether (**22a**) was replaced by 4-CF_3-phenol ether, however, still reduced the ability that inhibit C12-iE-DAP simulation of NOD1 signaling with the replacements of 4-CF_3 by 4-CN (**22f**) or 4-F (**22g**) too. It is noteworthy that a complete loss of antagonistic ability was observed for NOD1 signaling when R^4 was directly replaced by a 4-CN-phenyl (**22h**) or 4-CF_3-phenyl (**22i**) without an aliphatic linker.

In R^5, without 3-*N,N*-dimethylamino group, it resulted in significantly decreased their antagonistic activity, i.e. **22j**, **22k**. 2-*N,N*-dimethylamino (**22l**) or 4-*N,N*-dimethylamino (**22m**) substitution showed similar or less NOD1 antagonistic activities, respectively, in comparison with **14a**. It was interesting that replacement of *N,N*-dimethylamino with circinal morpholinyl group (**22n, 22o**) retained their high inhibitory percentage of NOD1 signaling. Since the benzylmethylene and *N,N*-dimethylamino in **14a** are potential metabolic sites, the metabolic stability of analogue **22o** was tested in mouse liver microsomes stability assessment. Unfortunately, it gained a short $T_{1/2}$ of 9.6 min.

The OMe ester of R^6 was then amidated by cyclohexylamines (Table 2). All collected analogues including **24a**-**24e** maintained high NOD1/2 inhibitory activity. Compound **24e** with IC_{50} values of 0.54 μM (NOD1) and 0.50 μM (NOD2) was chosen to test metabolic stability in mouse liver microsomes. Unfortunately, a short T1/2 (12.9 min) was observed.

Evaluation of **14b** analogues (Table 3) showed that compounds **22p**-**22t** without *N3*-substitution had relatively weak activity against NOD1/2, and their metabolic stability were not improved either (i.e. **22t**, $T_{1/2}$ = 10.1 min *in vitro*, IC_{50} = 2.48 μM for NOD1).

A series of 6-biphenyl-7-retroamide analogues of **14a** were designed and synthesized (Table 4) [23,24]. In R^5, we placed halogen atoms including F, Cl, and CF_3-substitutions to replace *N,N*-dimethylamino group. Compound **30d** bearing the 4-CF_3-phenol

Table 1
14a's derivatives at R^4 and R^5 [a].

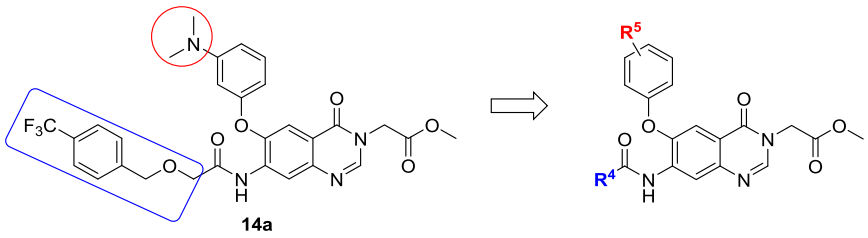

Compd.	R^4	R^5	NOD1/2 inhibition % [b]	IC_{50} (NOD1/2) μM ($T_{1/2}$) min [c]
14a	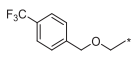	3-*N*,*N*-dimethylamino	85.44 ± 1.85/76.86 ± 1.62	1.15 ± 0.12/0.99 ± 0.06
22a	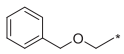	3-*N*,*N*-dimethylamino	47.61 ± 3.94/35.00 ± 3.14	ND
22b	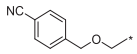	3-*N*,*N*-dimethylamino	55.69 ± 0.14/58.66 ± 1.29	ND
22c	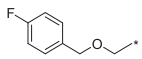	3-*N*,*N*-dimethylamino	33.38 ± 7.88/42.47 ± 18.76	ND
22d	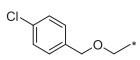	3-*N*,*N*-dimethylamino	69.03 ± 1.93/ND	4.31 ± 0.36/ND
22e	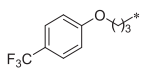	3-*N*,*N*-dimethylamino	70.88 ± 1.70/ND	2.65 ± 0.14/ND
22f	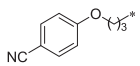	3-*N*,*N*-dimethylamino	48.04 ± 1.85/ND	ND
22g	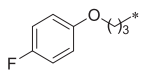	3-*N*,*N*-dimethylamino	33.46 ± 1.50/ND	ND
22h	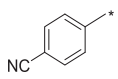	3-*N*,*N*-dimethylamino	13.06 ± 6.44/ND	ND
22i	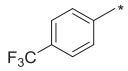	3-*N*,*N*-dimethylamino	31.70 ± 3.94/ND	ND
22j	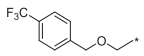	H	50.21 ± 0.85/ND	ND
22k	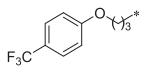	H	28.20 ± 6.71/ND	ND
22l	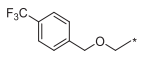	2-*N*,*N*-dimethylamino	87.86 ± 1.25/ND	1.65 ± 0.11/ND
22m	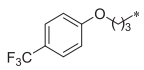	4-*N*,*N*-dimethylamino	68.37 ± 0.82/ND	3.87 ± 1.3/ND
22n	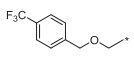	3-morpholinyl	88.92 ± 0.33/ND	0.65 ± 0.12/0.55 ± 0.05
22o	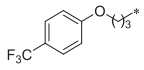	3-morpholinyl	91.17 ± 0.28/ND	1.38 ± 0.11/ND (9.6)

[a] All compounds were tested for C12-iE-DAP (50 ng/mL)-stimulated HEK-Blue hNOD1 cells and MDP (100 ng/mL)-stimulated HEK-Blue hNOD2 cells. ND: not determined.
[b] The compounds were tested at 5.0 μM.
[c] In mouse liver microsomes.

Table 2
14a's derivatives at R^5 and R^6 [a].

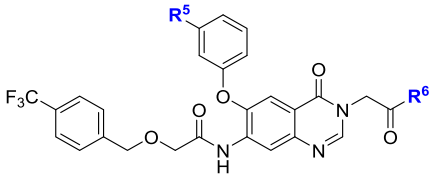

Compd.	R^5	R^6	NOD1/2 inhibition % [b]	IC_{50} (NOD1/2) μM ($T_{1/2}$) min [c]
14a		OMe	85.44 ± 1.85/76.86 ± 1.62	1.15 ± 0.12/0.99 ± 0.06
24a			87.48 ± 1.15/92.36 ± 0.45	0.26 ± 0.14/1.75 ± 0.20
24b			89.14 ± 1.18/94.35 ± 0.6	0.21 ± 0.12/1.11 ± 0.07
24c			82.01 ± 1.6/87 ± 0.69	0.27 ± 0.24/1.18 ± 0.17
24d			90.38 ± 1.66/94.15 ± 0.75	0.14 ± 0.17/0.66 ± 0.15
24e			88.25 ± 0.55/ND	0.54 ± 0.04/0.50 ± 0.05 (12.9)

[a] All compounds were tested for C12-iE-DAP (50 ng/mL)-stimulated HEK-Blue hNOD1 cells and MDP (100 ng/mL)-stimulated HEK-Blue hNOD2 cells. ND: not determined.
[b] The compounds were tested at 5.0 μM.
[c] In mouse liver microsomes.

ether group exhibited high NOD1 antagonistic activity, while substitutions with 4-chlorophenyl (**30b**) or phenyl (**30a** and **30c**) led to substantially decreased NOD1 inhibition. Interestingly, 3-chlorophenyl substitution in R^5 (**30a**-**30d**) showed higher NOD1 antagonistic activity compared with 3-fluorophenyl (**30e**-**30g**) or 3-CF_3-phenyl substitution (**30h**-**30j**). In R^3, replacement of H with glycine (**34a**-**34f**) showed similar NOD1 antagonistic activity. It was worth noting that incorporation of a free carboxylic acid group at *N3* position (**35**) resulted in a complete loss of NOD1/2 antagonistic activity possibly due to its negative charge which prevented the compound from interaction with NOD1/2 receptors [20]. It was again that *N3* piperidinyl amidation (**36a**) resulted in lowest IC_{50} values of 0.80 μM (NOD1) and 0.80 μM (NOD2), respectively, in this study. Compound **36a** showed a slightly improvement of metabolic stability *in vitro* with $T_{1/2}$ of 15.6 min, however, difluorination of the piperidyl group (**36b**) resulted in an acceptable $T_{1/2}$ of 67.6 min with dual NOD1/2 antagonistic activities for IC_{50} values of 1.13 μM (NOD1) and 0.77 μM (NOD2), respectively. Further investigations involved with pharmacokinetic studies *in vivo* will be developed as the reference for compound optimization.

A summary of SAR and SMR are shown in Fig. 3. It is firstly appeared that a free C2 position of the quinazolinone scaffold is necessary, for instance, any C2 substitution of the quinazolinone analogues, including alkylation, arylation, spiro- or fused quinazolinones, precludes antagonistic NOD1/2 signaling activity. Free *N3*-position decreased the activity in which an addition amidation is useful, in particular a difluorinated cyclohexylamine is optimal for its abilities of both acceptable IC_{50} values to NOD1/2 and metabolic stability in mouse microsomes. For the C6 position, phenoxy and phenyl substitutions show similar activities, and 3-*N,N*-dimethylamino, 3-morpholinyl and 3-halo aryl substituents all exhibit a comparable contribution, however, 3-halo aryl group is favor due to its metabolic stability in mouse liver microsomes. In the C7 position, the 4-CF_3-phenyl substituent and the alkoxy linker significantly contribute to the antagonistic activity. The retroamide fragment maintains antagonistic activity and slightly improves the metabolic stability. All results are clearly reflected in **36b** that is continuously investigated in next.

2.4. Biological profiling

The NOD1 and NOD2 inhibition effects of **36b** were dose-dependent, following a nonlinear semi logarithmic model (Fig. 4A). The sulforhodamine B (SRB) assay and interference test of SEAP (secreted embryonic alkaline phosphatase) were simultaneously performed to exclude cytotoxicity (Fig. 4B) and off targeted SEAP binding activity of **36b** (Fig. S1). Compound **36b** showed the promising inhibitory activity of both NOD1-and NOD2-induced NF-κB activation in HEK293 cells (IC_{50} = 1.13/0.77 μM, respectively) with no observed cytotoxicity at the tested concentrations.

Activation of NOD1 and NOD2 drives innate inflammatory responses that are primarily dependent on the activation of RIP2. The phosphorylation of RIP2 stimulates the NF-κB and MAPK signaling pathways and finally increases the release of cytokines in the macrophage, such as IL6, TNF-α and IL-8 [7]. To determine whether **36b** inhibited one or both of these pathways in a NOD1-or NOD2-dependent manner, the effect on total IkBα and phosphorylated IKKα/β, p65, p38, JNK and ERK levels were assessed in THP-1 cells with C12-iE-DAP or MDP stimulation, respectively (Fig. 5A and B). C12-iE-DAP at 500 ng/mL could induce NOD1 activation and resulted in increases of phospho-RIP2, phospho-p38, and phospho-JNK expression. A decrease in the level of IκBα and a barely

Table 3
14b derivatives of combined R^4, R^5 substituents [a].

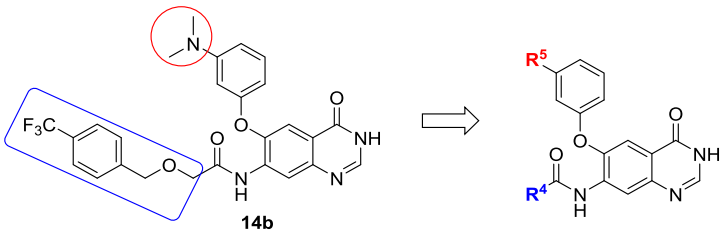

Compd.	R^4	R^5	NOD1/2 inhibition % [b]	IC_{50} (NOD1/2) μM ($T_{1/2}$) min [c]
14b	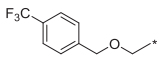		50.40 ± 0.54/53.96 ± 1.74	ND/0.80 ± 0.06
22p	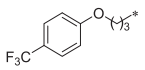		59.15 ± 1.41/58.52 ± 0.52	5.64 ± 2.33/4.77 ± 0.57
22q	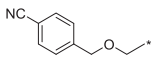		30.38 ± 19.43/19.33 ± 4.78	9.33/ND
22r	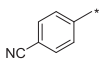		19.41 ± 5.64/13.11 ± 2.57	ND
22s	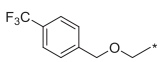		37.63 ± 3.98/ND	ND
22t	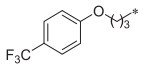		65.37 ± 1.36/ND	2.48 ± 0.39/ND (10.1)

[a] All compounds were tested for C12-iE-DAP (50 ng/mL)-stimulated HEK-Blue hNOD1 cells and MDP (100 ng/mL)-stimulated HEK-Blue hNOD2 cells. ND: not determined.
[b] The compounds were tested at 5.0 μM.
[c] In mouse liver microsomes.

discernible increase in phospho-ERK, consistent with our previous reports, were also observed [12,21]. Pretreatment of cells with **36b** at 1.0 μM and 10 μM prevented the increases in p-RIP2, p-IKKα/β, p-p65, p-p38, and p-JNK and the degradation of IκBα. Because C12-iE-DAP gave only weak induction of p-ERK, the reduction of these levels by **36b** was difficult to discern. Similarly, **36b** treatment markedly inhibited the MDP-induced phosphorylation of RIP2, IKKα/β, p65, p38 and JNK as well as the degradation of IκBα in a dose-dependent manner in THP-1 cells. Compound **36b** was also able to block NOD1-and NOD2-mediated inflammatory cytokine secretion in THP-1 cells. As shown in Fig. 5C and D, pretreatment of THP-1 cells with **36b** consistently and dose-dependently reduced the transcription of IL-6, TNF-α and IL-8 stimulated by C12-iE-DAP or MDP, respectively. These data suggest that **36b** inhibits both the NOD1 and NOD2 signaling pathways in human immune cells.

To determine whether **36b** affected similar sensitization of PTX *in vivo*, we tested the efficacy of PTX in combination with **36b** in B16 tumor-bearing mice that mimic human melanoma. As shown in Fig. 6, the combination therapy significantly reduced tumor growth compared with PTX treatment alone ($p < 0.001$), and the tumor weight inhibitory rate increased from 64.07% to 85.46%. Compared with the vehicle group, the combination of **36b** with PTX showed significant improvement in terms of therapeutic efficacy in B16-bearing mice.

3. Conclusions

In summary, two hit derivatives discovered by the screening of a quinazolinone focused library were found to show potential NOD1/2 antagonistic activities. Structural and metabolic site modifications led to the discovery of a dual NOD1/2 antagonist **36b** with its ability in significant improvement in terms of therapeutic efficacy in B16-bearing mice compared with PTX treatment alone. These results enrich the number of lead compounds in antagonizing NOD1/2 signaling for adjuvant cancer chemotherapy.

4. Experimental

4.1. General

THF, MeOH, DCM and other commercial reagents were purchased from domestic corporations and used without further purification. Silica gel for column chromatography and analytical thin layer chromatography (TLC) plates were phased from Qingdao Haiyang Chemical and Special Silica Gel Co, Ltd. The automatic LC-MS analysis was also performed on a Waters SQ Advantage mass spectrometer equipped with an UPLC system and an eluent splitter (5% eluent was split into the MS system). High-resolution LC-MS was carried out by Agilent LC/MSD TOF using a column of Agilent ZORBAX SB-C18 (rapid resolution, 3.5 μm, 2.1 × 30 mm) at a flow of 0.40 mL/min. The solvent was MeOH/water (75:25 (v/v)), containing 5 mmol/L ammonium formate. The ion source is electrospray ionization (ESI).

Proton nuclear magnetic resonance (^{1}H NMR) and carbon nuclear magnetic resonance (^{13}C NMR) spectroscopy were performed on Bruker Advance 400 NMR spectrometer. Unless otherwise noted

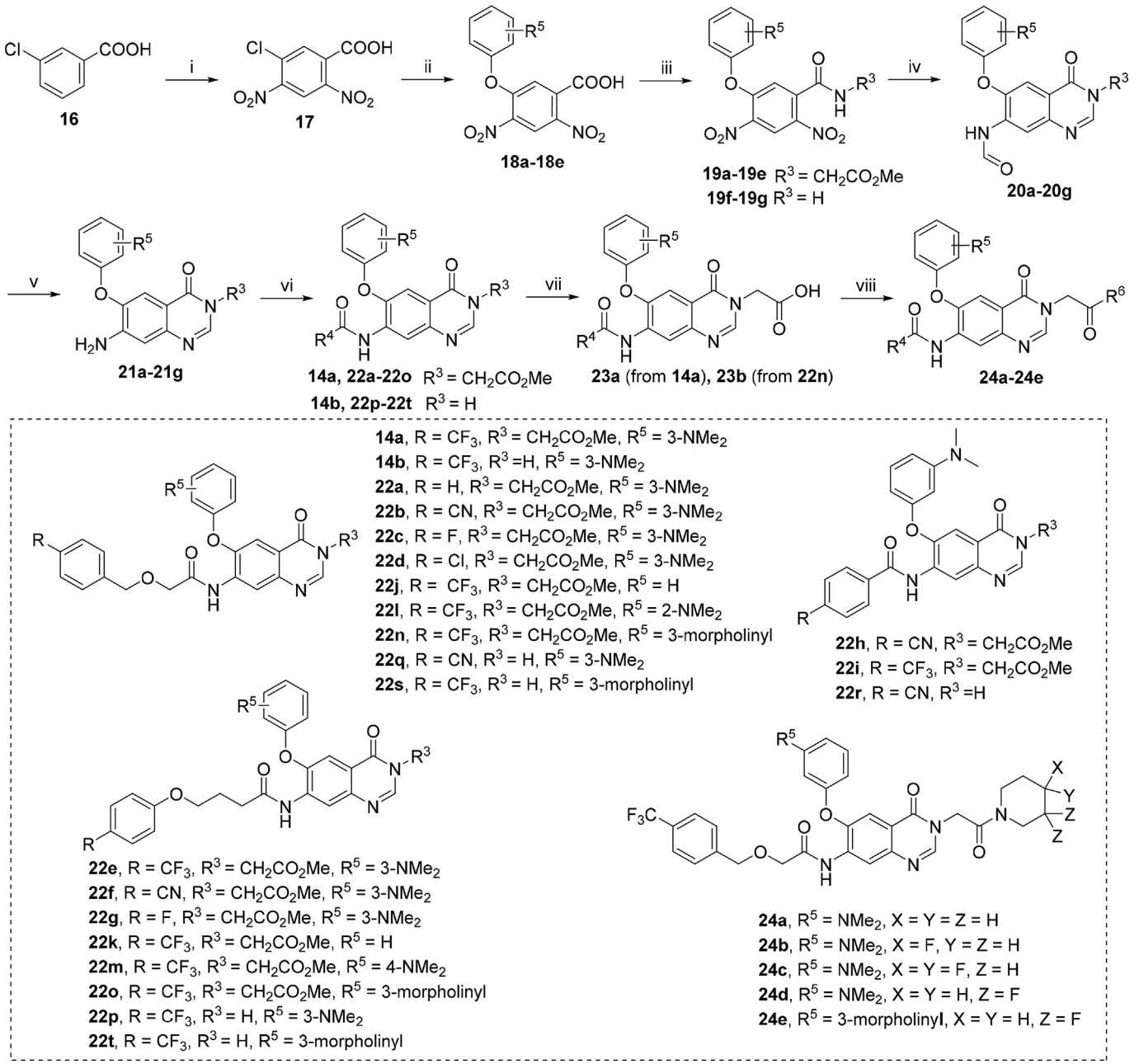

Scheme 1. Synthesis of quinazolinone derivatives. Reagents and conditions: (i) KNO_3, H_2SO_4, 80–130 °C, 6 h; (ii) phenol derivatives, $NaHCO_3$, H_2O, 110 °C, 2 h; (iii) methyl glycinate hydrochloride, or $NH_3 \cdot H_2O$, *N,N'*-diisopropylcarbodiimide (DIC), THF, rt; (iv) Fe, HCOOH, 100 °C, 5 h; (v) EtOH, concentrated HCl; (vi) acid chloride, Et_3N, THF; (vii) LiOH, THF/H_2O, 0.5 h; (viii) HOSu, DIC, amine derivatives THF; rt.

below, all compounds were >95% pure by analytical HPLC.

4.1.1. General procedure for the synthesis of compounds 14a, 14b, 20a-20t, 24a-24e (Scheme 1)

4.1.1.1. Synthesis of intermediate 17. To the solution of 3-chlorobenzoic acid **16** (20.0 g, 128.2 mmol) in sulfuric acid (240 mL), KNO_3 (33.0 g, 2.6 equiv.) was added by portions at room temperature. After KNO_3 was completely dissolved, the reaction mixture was heated to 80 °C and stirred 30 min s. After continuously stirred for at 2 h at 110 °C and at 130 °C respectively, the starting material was completely consumed. Then the reaction mixture was cooled to room temperature and poured into ice (660 g) slowly to afford the yellow solid which was collected by filtration and recrystallized with a mixed solution of EtOH and H_2O (EtOH/H_2O = 1:5) to give the intermediate **17** as yellow powder (44% yield). ^{1}H NMR (400 MHz, DMSO-d_6) δ 14.61 (s, 1H), 8.86 (s, 1H), 8.30 (s, 1H).

4.1.1.2. Synthesis of intermediates 18a-18e. To a solution of **17** (4.9 g, 19. 8 mmol) in H_2O (36 mL), $NaHCO_3$ (3. 6 g, 42.3 mmol) and phenol derivatives (1.1 equiv.) were added. The reaction mixture was heated to 110 °C and reflux for 2 h, then cooled to room temperature and treated with an aqueous solution of 6 N HCl at 0 °C to afford the crude intermediates (**18a-18e**) which were collected by filtration in 60%–70% yield. These compounds were dried and used for next step without further purification.

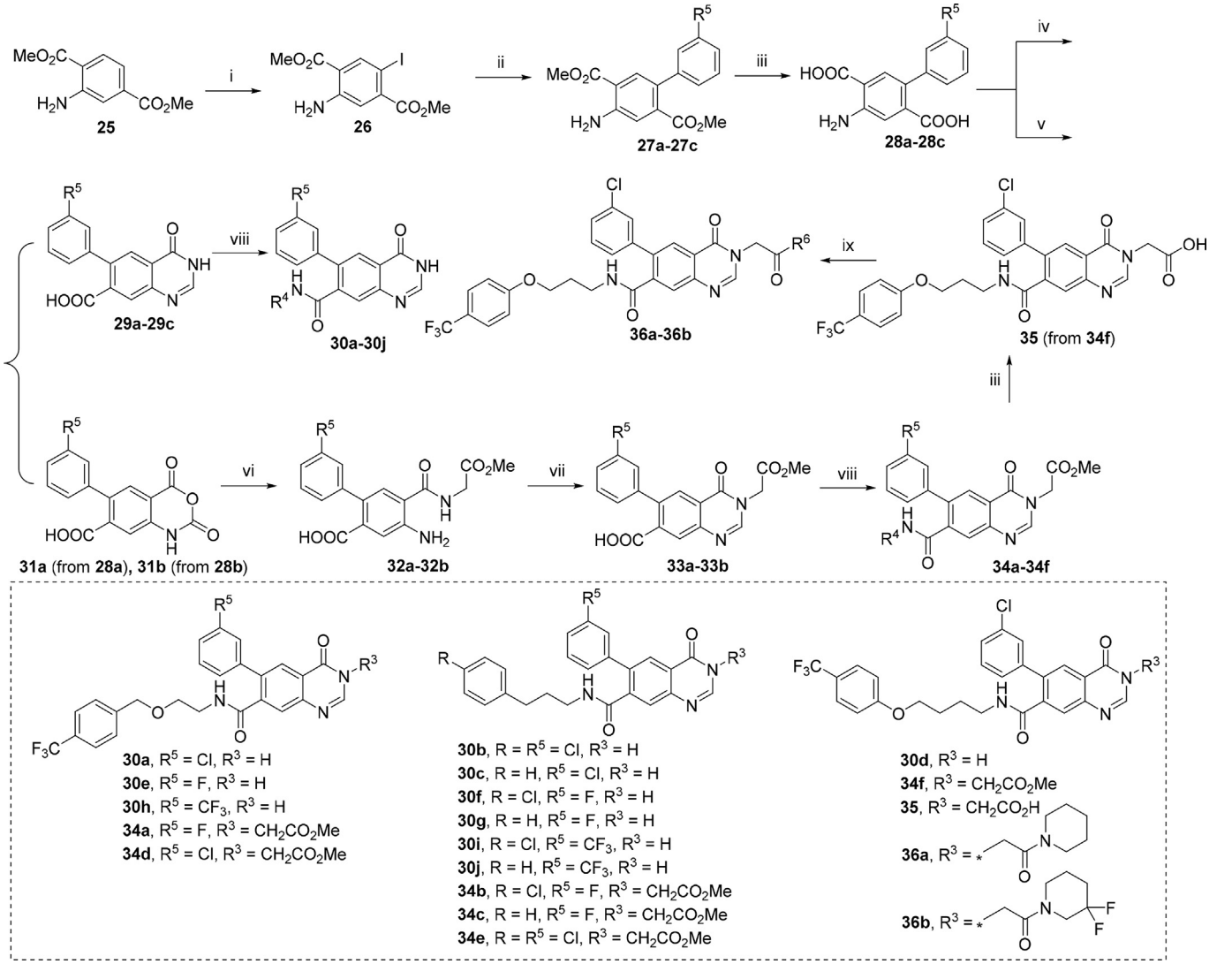

Scheme 2. Preparation of the retroamide quinazolinone analogues. Reagents and conditions: (i) *N*-iodosuccinimide, HOAc, rt, 24 h; (ii) phenylboronic acid derivatives, $Pd(PPh_3)_4$, Na_2CO_3, 80 °C; (iii) LiOH, THF/H_2O, 0.5 h; (iv) $HCONH_2$, 160 °C, 5 h; (v) triphosgene, THF, reflux; (vi) methyl glycinate hydrochloride, Et_3N, H_2O, rt; (vii) HCOOH, 110 °C, 5 h; (viii) amine derivatives, HATU; (ix) HOSu, DIC, amine derivatives THF; rt.

4.1.1.3. Synthesis of intermediates 19a-19g. To a solution of intermediates **18a-18e** (13.1 mmol) in THF (120 mL), amino acid hydrochloride (13.8 mmol, 1.1 equiv.) or aqueous ammonia (10 mL) and DIC (3.1 mL, 19.7 mmol) were added. The reaction mixture was stirred at room temperature for 4 h and filtered. The filtrate was concentrated and the reaction residue was dissolved in DCM and washed by water. The aqueous layer was extracted by DCM, the organic layer was combined and washed with brine and dried over anhydrous $MgSO_4$. DCM was then removed under reduced pressure and the residue was purified with flash column chromatography on silica gel to give the intermediates **19a-19g** in the yield of 70%–85%.

4.1.1.4. Synthesis of intermediates 20a-20g. To a solution of **19a-19g** (1.0 mmol) in acetic acid (10 mL), iron powder (20.0 mmol, 20 equiv.) was added. The reaction mixture was stirred at 90 °C for 1.5h–2.5 h, and cooled to room temperature. 20 mL of DCM was added, and the mixture was filtered. The filtrate was concentrated, and the residue was purified with flash column chromatography on silica gel to give the intermediates **20a-20g** in the yield of 30%–40%.

4.1.1.5. Synthesis of intermediates 21a-21g. To a solution of **20a-20g** (1 mmol) in EtOH (5 mL), conc. HCl (0.5 mL) was added. The reaction mixture was stirred at room temperature for 12 h. Then diethyl ether (50 mL) was added to give the white solid **21a-21g** in the yield of 70%–78%.

4.1.1.6. Synthesis of 14a, 14b, 22a-22t. To a solution of **21a-21g** (0.1 mmol) and triethylamine (69.6 μL, 0.5 mmol) in THF (4 mL), a mixture of acyl chlorides (0.2 mmol, 2 equiv.) in THF (1 mL) was added. The reaction mixture was stirred at room temperature for 0.5 h and concentrated under reduced pressure. The residue was purified with flash column chromatography on silica gel to give the compounds **14a, 14b, and 22a-22t** in the yield of 50%–88%.

4.1.1.6.1. Methyl 2-(6-(3-(dimethylamino)phenoxy)-4-oxo-7-(2-((4-(trifluoromethyl)benzyl) oxy)acetamido)quinazolin-3(4H)-yl)acetate (14a). Yellow powder (78% yield), mp: 165–166 °C. ^{1}H NMR (400 MHz, DMSO-d_6) δ 9.67 (s, 1H), 8.66 (s, 1H), 8.30 (s, 1H), 7.57 (s, 4H), 7.36 (s, 1H), 7.27–7.23 (m, 1H), 6.64 (dd, J = 8.4, 1.9 Hz, 1H), 6.53 (s, 1H), 6.38 (dd, J = 7.9, 1.5 Hz, 1H), 4.78–4.76 (m, 4H), 4.33 (s, 2H), 3.68 (s, 3H), 2.89 (s, 6H). ^{13}C NMR (100 MHz, DMSO-d_6) δ 168.5,

Table 4
6-Biphenyl-7-retroamide analogues [a].

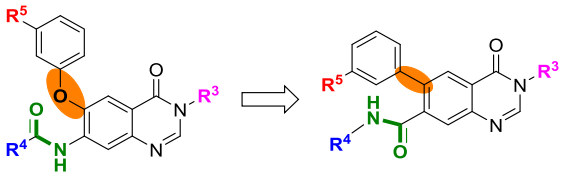

Compd.	R^5	R^4	R^3	NOD1/2 inhibition % [b]	IC_{50} (NOD1/2) μM ($T_{1/2}$) min [c]
30a	Cl	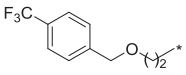	H	64.36 ± 1.11/ND	1.34 ± 0.33/ND (22.9 min)
30b	Cl	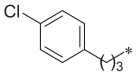	H	41.48 ± 4.17/ND	ND
30c	Cl	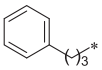	H	6.60 ± 6.10/ND	ND
30d	Cl	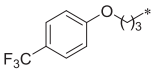	H	89.96 ± 0.23/ND	0.84 ± 0.08/0.84 ± 0.09
30e	F	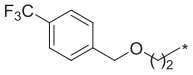	H	56.14 ± 1.45/ND	4.11 ± 0.62/ND
30f	F	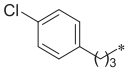	H	43.51 ± 4.18/ND	ND
30g	F	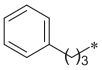	H	−1.81 ± 8.27/ND	ND
30h	CF_3	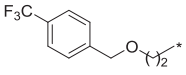	H	72.44 ± 1.86/ND	4.39 ± 0.45/ND
30i	CF_3	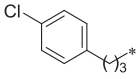	H	34.95 ± 2.41/ND	ND
30j	CF_3	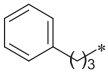	H	4.06 ± 3.59/ND	ND
34a	F	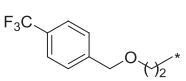		64.04 ± 1.84/ND	3.46 ± 0.27/ND
34b	F	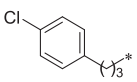		65.31 ± 1.53/ND	3.24 ± 0.30/ND
34c	F	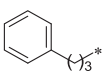		−0.98 ± 8.22/ND	ND
34d	Cl	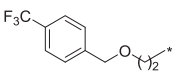		82.36 ± 0.6/ND	1.12 ± 0.20/ND
34e	Cl	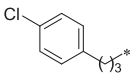		58.17 ± 1.89/ND	1.64 ± 0.44/ND

(*continued on next page*)

Table 4 (*continued*)

Compd.	R^5	R^4	R^3	NOD1/2 inhibition % [b]	IC_{50} (NOD1/2) μM ($T_{1/2}$) min [c]
34f	Cl	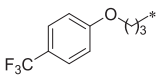		89.62 ± 0.53/ND	0.89 ± 0.09/1.00 ± 0.07
35	Cl	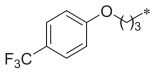		21.97 ± 6.91/ND	ND
36a	Cl	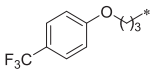		93.25 ± 0.40/ND	0.80 ± 0.08/0.80 ± 0.10 (15.6)
36b	Cl	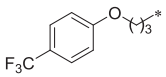	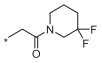	91.37 ± 0.65/ND	1.13 ± 0.13/0.77 ± 0.09 (67.7)

[a] All compounds were tested for C12-iE-DAP (50 ng/mL)-Stimulated HEK-Blue hNOD1 Cells and MDP (100 ng/mL)-Stimulated HEK-Blue hNOD2 Cells. ND: not determined.
[b] The compounds were tested at 5.0 μM.
[c] In mouse liver microsomes.

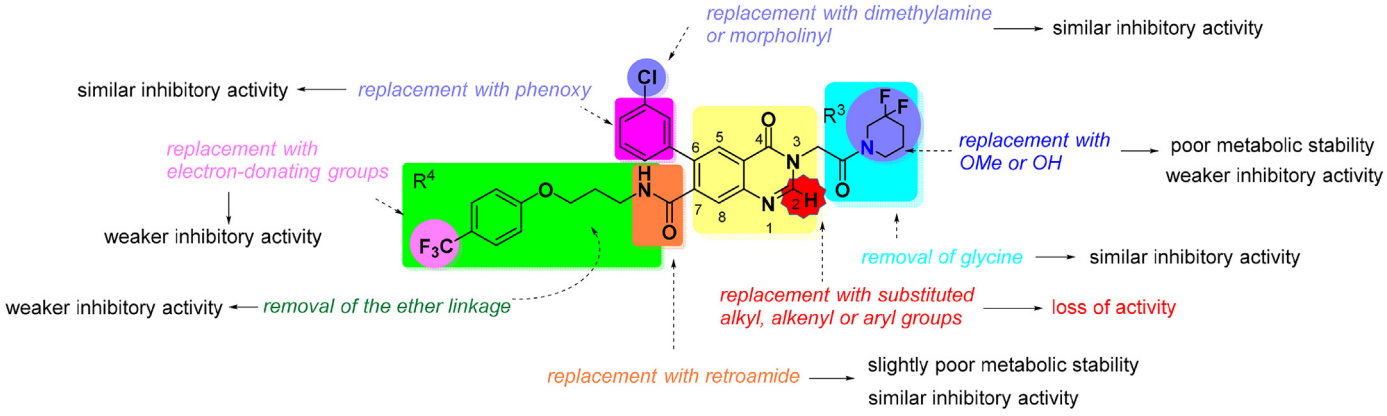

Fig. 3. SAR and SMR's summary of quinazolinone derivatives.

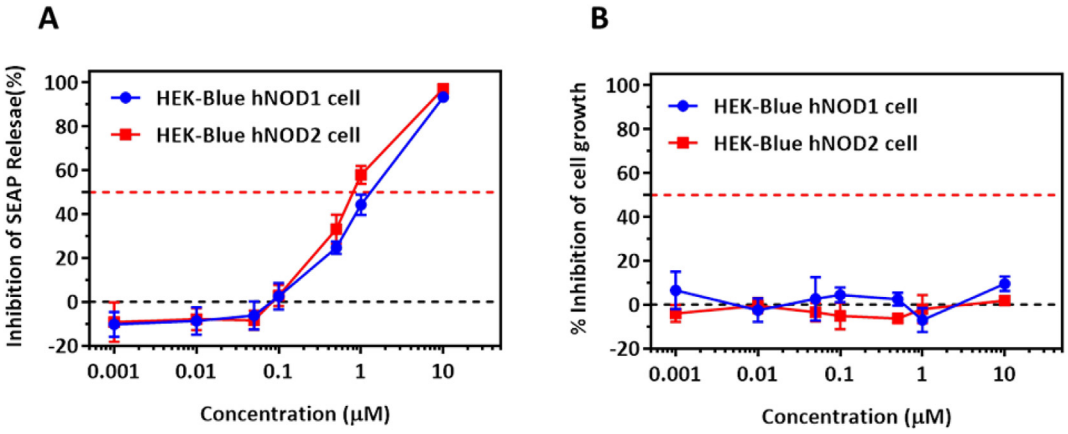

Fig. 4. (A) Compound **36b** inhibits C12-iE-DAP-induced or MDP-induced NF-κB activation. HEK-Blue hNOD1 and HEK-Blue hNOD2 cells were preincubated with different concentrations of **36b** for 3 h and then stimulated with C12-iE-DAP (50 ng/mL) and MDP (100 ng/mL) for an additional 20 h. SEAP was quantified as described in the Experimental Section. Data are presented as the mean ± standard deviation (SD) (n = 3). **(B)** Compound **36b** had no or little effect on cell growth. Following SEAP quantification, cells were fixed with 80% TCA at 4 °C for 1 h and stained with SRB in 1% acetic acid for 10 min. Then, the plates were washed five times and air-dried at room temperature (r.t.). Bound stain was subsequently solubilized with 10 mM Tris base (150 μL), and the absorbance was measured with a spectrophotometer at 515 nm. The inhibition rate of cell growth was calculated by the following formula: [(C−T)/C] × 100 (C, OD of control group; T, OD of compound-treated group). Data are shown as the mean ± SD (n = 3).

168.4, 159.2, 155.8, 152.2, 147.2, 146.6, 144.3, 142.3, 134.2, 130.4, 128.3, 128.0, 127.8, 125.1 (q, J = 3.7 Hz), 116.9, 116.7, 110.6, 109.1, 106.6, 103.6, 71.6, 69.7, 52.4, 47.1, 39.9. HRMS (ESI): m/z ($M + H^+$) calcd for $C_{29}H_{28}F_3N_4O_6$, 585.1956, found: 585.1950.

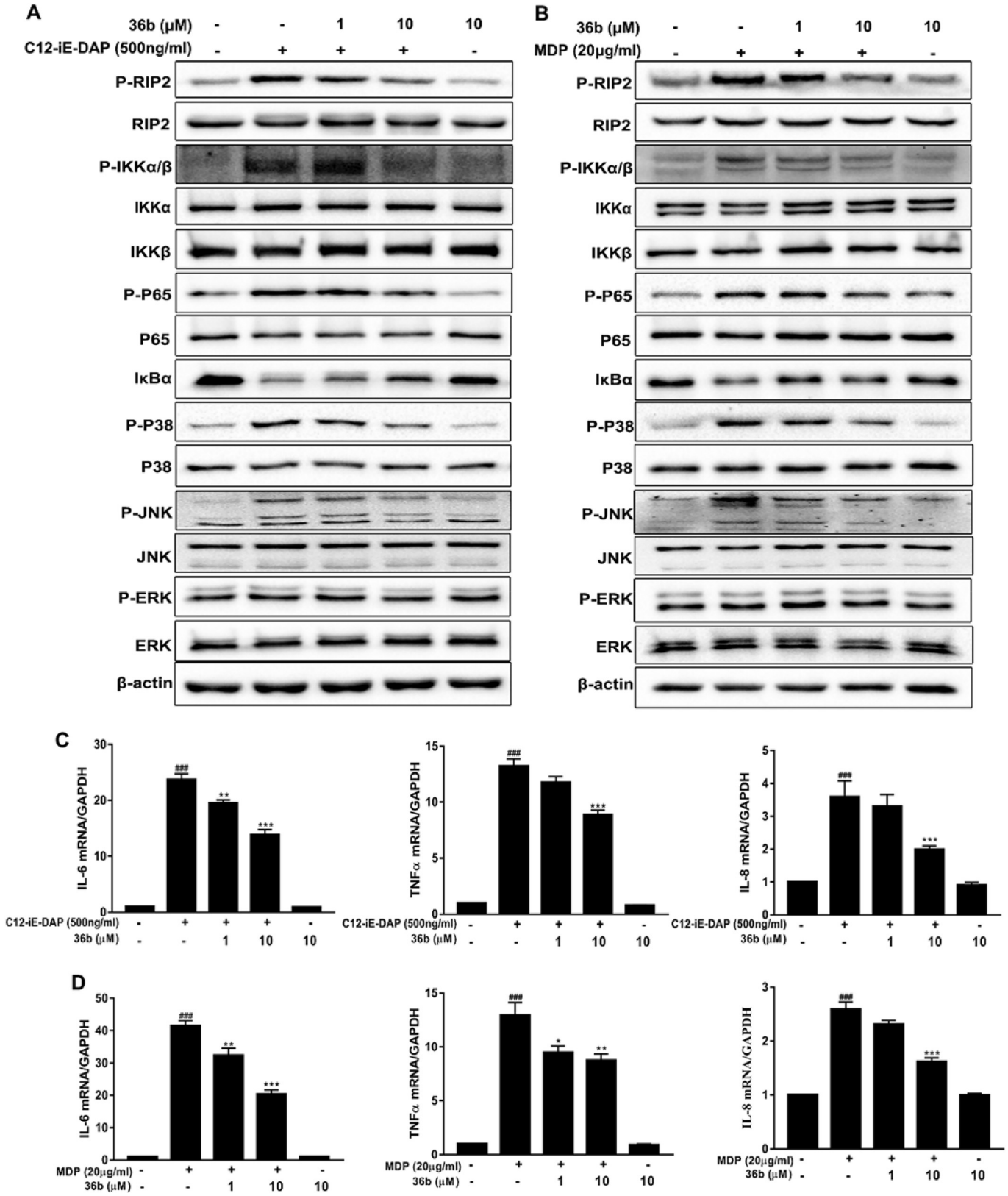

Fig. 5. Compound **36b** suppresses inflammation via NOD1 and NOD2 activation. Serum-starved THP1 cells were pretreated with or without **36b** (1.0 μM or 10 μM) for 1 h prior to (A) C12-iE-DAP (500 ng/mL) or (B) MDP (20 μg/mL) treatment for 30 min. The levels of IκBα and total and phosphorylated RIP2, IKKα/β, p65, JNK, p38, and ERK1/2 were determined by Western blotting. β-Actin was used as a loading control. (C, D) THP-1 cells were treated with or without **36b** (1.0 μM or 10 μM) for 1 h and then stimulated with (C) C12-iE-DAP (500 ng/mL) or (D) MDP (20 μg/mL) for 90 min. The mRNA levels of IL-6, TNF-α and IL-8 were determined by qRT-PCR. Data are presented as the mean ± standard deviation (SD) (n = 6): (*) $p < 0.05$, (**) $p < 0.01$, (***) $p < 0.001$ vs C12-iE-DAP- or MDP-treated group; (#) $p < 0.05$, (##) $p < 0.01$, (###) $p < 0.001$ vs the vehicle group.

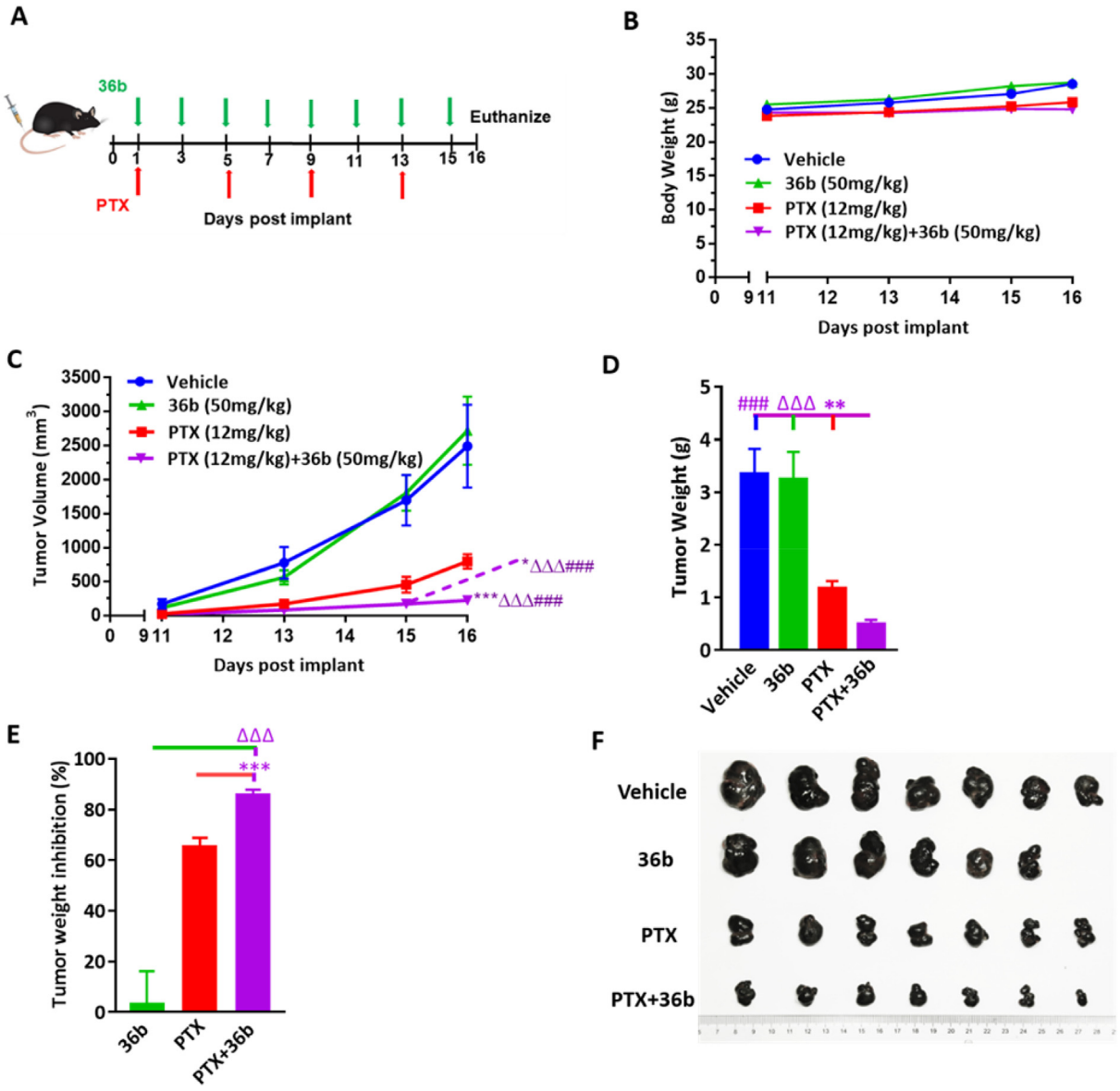

Fig. 6. Compound **36b** improves the antitumor efficacy of PTX in B16 tumor-bearing model. (A) Schematic timeline and treatment for **36b** and PTX in B16 tumor-bearing model. (B) Compound **36b** has no effect on the body weight of mice. (C) Compound **36b** improves the efficacy of PTX in inhibiting B16 tumor growth. 11 days after tumor implantation, tumor volumes were measured and presented as the mean ± SEM ($n \geq 6$). (D) Mice were sacrificed and tumors were removed and weighed. (E) Tumor weight inhibition rate was calculated by the following formula: $[(C - T)/C] \times 100$ (C, tumor weight of vehicle group; T, tumor weight of treated group). (F) Image of the tumors. Data are shown as the mean ± SEM: (*) $p < 0.05$, (**) $p < 0.01$, (***) $p < 0.001$ vs the PTX group; (△) $p < 0.05$, (△△) $p < 0.01$, (△△△) $p < 0.001$ vs **36b** group; (#) $p < 0.05$, (##) $p < 0.01$, (###) $p < 0.001$ vs the vehicle group.

4.1.1.6.2. N-(6-(3-(dimethylamino)phenoxy)-4-oxo-3,4-dihydroquinazolin-7-yl)-2-((4-(trifluoromethyl)benzyl)oxy)acetamide (14b). White powder (72% yield), mp: 191–192 °C. ^{1}H NMR (400 MHz, DMSO-d_6) δ 12.20 (br s, 1H), 9.62 (s, 1H), 8.61 (s, 1H), 8.03 (s, 1H), 7.56 (s, 4H), 7.35 (s, 1H), 7.2–7.23 (m, 1H), 6.63 (dd, J = 8.1, 1.6 Hz, 1H), 6.51 (s, 1H), 6.37 (d, J = 8.1 Hz, 1H), 4.75–4.72 (m, 2H), 4.32–4.29 (m, 2H), 2.89 (s, 6H). ^{13}C NMR (101 MHz, DMSO-d_6) δ 168.4, 159.9, 156.0, 152.2, 146.2, 144.8, 142.3, 133.8, 130.4, 129.7, 127.9, 127.8, 125.1 (d, J = 3.9 Hz), 118.1, 116.9, 110.6, 109.0, 106.6, 103.6, 103.6, 71.6, 69.7. HRMS (ESI): m/z (M + H$^+$) calcd for $C_{26}H_{24}O_4N_4F_3$, 513.1744, found: 513.1742.

4.1.1.6.3. Methyl 2-(7-(2-(benzyloxy)acetamido)-6-(3-(dimethylamino)phenoxy)-4-oxo quinazolin-3(4H)-yl)acetate (22a). Red powder (78% yield), mp: 155–156 °C. ^{1}H NMR (400 MHz, DMSO-d_6) δ 9.63 (s, 1H), 8.66 (s, 1H), 8.30 (s, 1H), 7.37–7.35 (m, 2H), 7.33 (s, 1H), 7.27 (dd, J = 10.1, 6.2 Hz, 4H), 6.65 (dd, J = 8.3, 1.9 Hz, 1H), 6.54 (s, 1H), 6.41 (dd, J = 7.9, 1.6 Hz, 1H), 4.78 (s, 2H), 4.65 (s, 2H), 4.27 (s, 2H), 3.68 (s, 3H), 2.90 (s, 6H). ^{13}C NMR (100 MHz, DMSO-d_6) δ 168.7, 168.4, 159.2, 155.7, 152.2, 147.2, 146.7, 144.3, 137.2, 134.1, 130.5, 128.3, 127.8, 127.7, 116.8, 116.6, 110.4, 109.2, 106.8, 103.7, 72.7, 69.4, 52.4, 47.1. HRMS (ESI): m/z (M + H$^+$) calcd for $C_{28}H_{29}N_4O_6$, 517.2082, found: 517.2081.

4.1.1.6.4. Methyl 2-(7-(2-((4-cyanobenzyl)oxy)acetamido)-6-(3-(dimethylamino)phenoxy)- 4-oxo quinazolin-3(4H)-yl)acetate (22b). White powder (80% yield), mp: 199–200 °C. ^{1}H NMR (400 MHz, DMSO-d_6) δ 9.64 (s, 1H), 8.64 (s, 1H), 8.30 (s, 1H), 7.68 (d, J = 8.1 Hz, 2H), 7.55 (d, J = 8.1 Hz, 2H), 7.35 (s, 1H), 7.28–7.23 (m, 1H), 6.64 (dd, J = 8.3, 2.1 Hz, 1H), 6.49–6.47 m, 1H), 6.36 (dd, J = 7.9, 1.8 Hz, 1H), 4.78 (s, 2H), 4.75 (s, 2H), 4.33 (s, 2H), 3.68 (s, 3H), 2.90 (s, 6H). ^{13}C NMR (101 MHz, DMSO-d_6) δ 168.5, 168.4, 159.2, 155.8, 152.2, 147.2,

146.7, 144.3, 143.2, 134.2, 132.2, 130.4, 127.9, 118.7, 117.0, 116.7, 110.7, 110.3, 109.1, 106.6, 103.6, 71.6, 69.7, 52.4, 47.1. HRMS (ESI): *m/z* ($M + H^+$) calcd for $C_{29}H_{28}N_5O_6$, 542.2010, found: 542.2013.

4.1.1.6.5. Methyl 2-(6-(3-(dimethylamino)phenoxy)-7-(2-((4-fluorobenzyl)oxy)acetamido)- 4-oxoquinazolin-3(4H)-yl)acetate (22c). White powder (85% yield), mp: 173–174 °C. ^{1}H NMR (400 MHz, DMSO-d_6) δ 9.62 (s, 1H), 8.65 (s, 1H), 8.29 (s, 1H), 7.33 (s, 1H), 7.31–7.24 (m, 2H), 7.23–7.18 (m, 2H), 7.14–7.05 (m, 1H), 6.63 (dd, *J* = 8.3, 2.1 Hz, 1H), 6.53–6.4 (m, 1H), 6.39 (dd, *J* = 7.9, 1.9 Hz, 1H), 4.78 (s, 2H), 4.67 (s, 2H), 4.29 (s, 2H), 3.68 (s, 3H), 2.90 (s, 6H). ^{13}C NMR (101 MHz, DMSO-d_6) δ 168.6, 168.4, 162.1 (d, *J* = 243.8 Hz), 159.2, 155.7, 152.2, 147.2, 146.8, 144.2, 140.3 (d, *J* = 7.3 Hz), 134.1, 130.4, 130.2 (d, *J* = 8.3 Hz), 123.4 (d, *J* = 2.7 Hz), 117.0, 116.6, 114.5 (d, *J* = 21.0 Hz), 114.1 (d, *J* = 21.6 Hz), 110.4, 109.2, 106.8, 103.7, 71.8, 69.5, 52.4, 47.1. HRMS (ESI): *m/z* ($M + H^+$) calcd for $C_{28}H_{28}FN_4O_6$, 535.1987, found: 535.1989.

4.1.1.6.6. Methyl 2-(7-(2-((4-chlorobenzyl)oxy)acetamido)-6-(3-(dimethylamino)phenoxy)- 4-oxoquinazolin-3(4H)-yl)acetate (22d). White powder (83% yield), mp: 148–149 °C. ^{1}H NMR (400 MHz, DMSO-d_6) δ 9.62 (s, 1H), 8.66 (s, 1H), 8.30 (s, 1H), 7.36 (d, *J* = 8.4 Hz, 3H), 7.27 (d, *J* = 8.2 Hz, 3H), 6.65 (dd, *J* = 8.4, 2.1 Hz, 1H), 6.52 (t, *J* = 2.2 Hz, 1H), 6.38 (dd, *J* = 7.9, 1.8 Hz, 1H), 4.78 (s, 2H), 4.64 (s, 2H), 4.28 (s, 2H), 3.68 (s, 3H), 2.91 (s, 6H). ^{13}C NMR (101 MHz, DMSO-d_6) δ 168.6, 168.4, 159.2, 155.8, 152.2, 147.2, 146.7, 144.3, 136.4, 134.1, 132.3, 130.5, 129.4, 128.3, 116.8, 116.6, 110.6, 109.1, 106.7, 103.6, 71.7, 69.5, 52.4, 47.1. HRMS (ESI): *m/z* ($M + H^+$) calcd for $C_{28}H_{28}ClN_4O_6$, 551.1692, found: 551.1696.

4.1.1.6.7. Methyl 2-(6-(3-(dimethylamino)phenoxy)-4-oxo-7-(4-(4-(trifluoromethyl)phenoxy) butanamido)quinazolin-3(4H)-yl)acetate (22e). White powder (82% yield), mp: 161–165 °C. ^{1}H NMR (400 MHz, DMSO-d_6) δ 9.92 (s, 1H), 8.59 (s, 1H), 8.26 (s, 1H), 7.63 (d, *J* = 8.7 Hz, 2H), 7.27 (s, 1H), 7.27–7.21 (m, 1H), 7.10 (d, *J* = 8.6 Hz, 2H), 6.62 (dd, *J* = 8.3, 2.2 Hz, 1H), 6.51–6.48 (m, 1H), 6.36 (dd, *J* = 7.8, 1.9 Hz, 1H), 4.77 (s, 2H), 4.12 (t, *J* = 6.3 Hz, 2H), 3.67 (s, 3H), 2.90 (s, 6H), 2.74–2.70 (m, 2H), 2.07 (dd, *J* = 13.7, 6.8 Hz, 2H). ^{13}C NMR (101 MHz, DMSO-d_6) δ 172.1, 168.4, 161.4, 161.1, 159.2, 156.0, 152.1, 147.7, 146.9, 145.5, 144.0, 135.2, 130.3, 126.9 (q, *J* = 3.7 Hz), 118.4, 116.4, 114.9, 110.2, 109.0, 107.3, 104.1, 67.4, 52.4, 47.1, 32.8, 24.4. HRMS (ESI): *m/z* ($M + H^+$) calcd for $C_{30}H_{20}F_3N_4O_6$, 599.2112, found: 599.2114.

4.1.1.6.8. Methyl 2-(7-(4-(4-cyanophenoxy)butanamido)-6-(3-(dimethylamino)phenoxy)- 4-oxoquinazolin-3(4H)-yl)acetate (22f). Yellow powder (71% yield), mp: 124–125 °C. ^{1}H NMR (400 MHz, DMSO-d_6) δ 9.91 (s, 1H), 8.59 (s, 1H), 8.26 (s, 1H), 7.74 (d, *J* = 8.8 Hz, 2H), 7.27 (s, 1H), 7.23 (d, *J* = 8.1 Hz, 1H), 7.09 (d, *J* = 8.8 Hz, 2H), 6.61 (dd, *J* = 8.4, 2.1 Hz, 1H), 6.49 (t, *J* = 2.1 Hz, 1H), 6.36 (dd, *J* = 7.9, 1.7 Hz, 1H), 4.77 (s, 2H), 4.13 (t, *J* = 6.3 Hz, 2H), 3.67 (s, 3H), 2.90 (s, 6H), 2.72 (t, *J* = 7.2 Hz, 2H), 2.08 (dd, *J* = 13.4, 6.7 Hz, 2H). ^{13}C NMR (101 MHz, DMSO-d_6) δ 172.1, 168.4, 162.0, 159.2, 156.0, 152.1, 147.7, 146.9, 144.0, 135.2, 134.2, 130.3, 119.2, 118.4, 116.4, 115.5, 110.2, 109.0, 107.3, 104.1, 102.7, 67.5, 52.4, 47.1, 40.0, 32.7, 24.3. HRMS (ESI): *m/z* ($M + H^+$) calcd for $C_{30}H_{30}N_5O_6$, 556.2191, found: 556.2193.

4.1.1.6.9. Methyl 2-(6-(3-(dimethylamino)phenoxy)-7-(4-(4-fluorophenoxy)butanamido)- 4-oxoquinazolin-3(4H)-yl)acetate (22g). White powder (80% yield), mp: 201–202 °C. ^{1}H NMR (400 MHz, DMSO-d_6) δ 9.90 (s, 1H), 8.59 (s, 1H), 8.26 (s, 1H), 7.28–7.22 (m, 2H), 7.08 (dd, *J* = 10.9, 4.4 Hz, 2H), 6.95–6.91 (m, 2H), 6.62 (dd, *J* = 8.4, 2.3 Hz, 1H), 6.51–6.49 (m, 1H), 6.37 (dd, *J* = 7.9, 2.0 Hz, 1H), 4.77 (s, 2H), 3.99 (t, *J* = 6.3 Hz, 2H), 3.67 (s, 3H), 2.90 (s, 6H), 2.70 (t, *J* = 7.3 Hz, 2H), 2.06–2.01 (m, 2H). ^{13}C NMR (101 MHz, DMSO-d_6) δ 172.2, 168.4, 159.2, 156.0, 152.1, 147.7, 146.9, 144.0, 135.2, 130.3, 118.4, 116.3, 115.9, 115.7, 115.7, 115.6, 110.2, 109.0, 107.3, 104.2, 67.5, 52.4, 47.1, 32.9, 24.6. HRMS (ESI): *m/z* ($M + H^+$) calcd for $C_{29}H_{29}FN_4O_6$, 549.2144, found: 549.2146.

4.1.1.6.10. Methyl 2-(7-(4-cyanobenzamido)-6-(3-(dimethylamino)phenoxy)-4-oxoquinazolin −3(4H)-yl)acetate (22 h). Yellow powder (78% yield), mp: 178–180 °C. ^{1}H NMR (400 MHz, DMSO-d_6) δ 10.36 (s, 1H), 8.34 (d, *J* = 19.6 Hz, 2H), 8.07 (d, *J* = 8.3 Hz, 2H), 8.02 (d, *J* = 8.3 Hz, 2H), 7.40 (s, 1H), 7.26–7.21 (m, 1H), 6.60 (dd, *J* = 8.3, 2.0 Hz, 1H), 6.51 (s, 1H), 6.39 (dd, *J* = 7.9, 1.5 Hz, 1H), 4.80 (s, 2H), 3.69 (s, 3H), 2.89 (s, 6H). ^{13}C NMR (101 MHz, DMSO-d_6) δ 168.4, 164.8, 159.2, 156.1, 152.1, 149.3, 147.1, 143.8, 138.2, 134.6, 132.5, 130.3, 128.7, 121.6, 118.2, 118.1, 114.2, 111.2, 108.9, 107.0, 103.8, 52.4, 47.2. HRMS (ESI): *m/z* ($M + H^+$) calcd for $C_{27}H_{24}N_5O_5$, 498.1772, found: 498.1771.

4.1.1.6.11. Methyl 2-(6-(3-(dimethylamino)phenoxy)-4-oxo-7-(4-(trifluoromethyl)benzamido) quinazolin-3(4H)-yl)acetate (22i). Yellow powder (70% yield), mp: 190–192 °C. ^{1}H NMR (400 MHz, DMSO-d_6) δ 10.32 (s, 1H), 8.35 (d, *J* = 28.7 Hz, 2H), 8.11 (d, *J* = 8.0 Hz, 2H), 7.91 (d, *J* = 8.2 Hz, 2H), 7.40 (s, 1H), 7.26–7.20 (m, 1H), 6.60 (dd, *J* = 8.4, 1.8 Hz, 1H), 6.52 (s, 1H), 6.40 (d, *J* = 7.9 Hz, 1H), 4.80 (s, 2H), 3.69 (s, 3H), 2.88 (s, 6H). ^{13}C NMR (101 MHz, DMSO-d_6) δ 168.4, 165.0, 159.3, 156.1, 152.1, 149.3, 147.1, 143.8, 138.0, 134.6, 131.5, 130.3, 128.8, 125.4 (dd, *J* = 7.4, 3.6 Hz), 122.5, 121.4, 118.0, 111.1, 108.9, 107.0, 103.9, 52.4, 47.2. HRMS (ESI): *m/z* ($M + H^+$) calcd for $C_{27}H_{24}F_3N_4O_5$, 541.1693, found: 541.1697.

4.1.1.6.12. Methyl2-(4-oxo-6-phenoxy-7-(2-((4-(trifluoromethyl) benzyl)oxy)acetamido) quinazolin-3(4H)-yl)acetate (22j). Yellow powder (80% yield), mp: 170–172 °C. ^{1}H NMR (400 MHz, DMSO-d_6) δ 9.70 (s, 1H), 8.67 (s, 1H), 8.32 (s, 1H), 7.65–7.54 (m, 4H), 7.51–7.45 (m, 2H), 7.35–7.25 (m, 2H), 7.19 (d, *J* = 7.7 Hz, 2H), 4.76 (d, *J* = 17.1 Hz, 4H), 4.33 (s, 2H), 3.68 (s, 3H). ^{13}C NMR (101 MHz, DMSO-d_6) δ 168.6, 168.4, 159.2, 155.0, 147.5, 146.4, 144.6, 142.3, 134.5, 130.5, 128.4, 128.0, 125.6, 125.1 (q, *J* = 3.7 Hz), 122.9, 119.9, 117.2, 116.7, 111.0, 71.7, 69.8, 52.4, 47.2. HRMS (ESI): *m/z* ($M + H^+$) calcd for $C_{27}H_{23}F_3N_3O_6$, 542.1534, found: 542.1536.

4.1.1.6.13. Methyl 2-(4-oxo-6-phenoxy-7-(4-(4-(trifluoromethyl) phenoxy)butanamido) quinazolin-3(4H)-yl)acetate (22k). White powder (78% yield), mp: 152–154 °C. ^{1}H NMR (400 MHz, DMSO-d_6) δ 9.99 (s, 1H), 8.62 (s, 1H), 8.29 (s, 1H), 7.63 (d, *J* = 8.7 Hz, 2H), 7.50–7.44 (m, 2H), 7.29–7.24 (m, 2H), 7.16 (d, *J* = 7.8 Hz, 2H), 7.10 (d, *J* = 8.6 Hz, 2H), 4.77 (s, 2H), 4.11 (t, *J* = 6.3 Hz, 2H), 3.68 (s, 3H), 2.72 (t, *J* = 7.2 Hz, 2H), 2.11–2.02 (m, 2H). ^{13}C NMR (101 MHz, DMSO-d_6) δ 172.1, 168.4, 161.4, 159.2, 155.3, 147.2 (d, *J* = 7.1 Hz), 144.4, 135.6, 130.3, 126.9 (q, *J* = 3.7 Hz), 125.9, 124.9, 123.2, 121.6, 120.2, 118.7, 116.4, 114.9, 111.0, 67.3, 52.4, 47.1, 32.8, 24.4. HRMS (ESI): *m/z* ($M + H^+$) calcd for $C_{28}H_{25}F_3N_3O_6$, 556.1690, found: 556.1677.

4.1.1.6.14. Methyl 2-(6-(2-(dimethylamino)phenoxy)-4-oxo-7-(2-((4-(trifluoromethyl)benzyl) oxy)acetamido)quinazolin-3(4H)-yl)acetate (22l). Red powder (59% yield), mp: 62–64 °C. ^{1}H NMR (400 MHz, DMSO-d_6) δ 9.77 (s, 1H), 8.67 (s, 1H), 8.29 (s, 1H), 7.57 (d, *J* = 6.7 Hz, 4H), 7.26 (dd, *J* = 11.2, 4.1 Hz, 1H), 7.12 (dd, *J* = 8.1, 1.4 Hz, 2H), 7.07 (s, 1H), 7.03 (dd, *J* = 10.8, 4.4 Hz, 1H), 4.77 (d, *J* = 5.4 Hz, 4H), 4.37 (s, 2H), 3.67 (s, 3H), 2.61 (s, 6H). ^{13}C NMR (101 MHz, DMSO-d_6) δ 168.5, 168.4, 159.2, 147.1, 146.4, 145.2, 145.2, 144.0, 142.3, 133.6, 129.6, 128.0, 126.6, 125.5, 125.1 (q, *J* = 3.7 Hz), 122.6, 121.9, 119.1, 116.7, 116.6, 108.6, 71.7, 69.7, 52.4, 47.1, 42.6. HRMS (ESI): *m/z* ($M + H^+$) calcd for $C_{29}H_{28}F_3N_4O_6$, 585.1956, found: 585.1954.

4.1.1.6.15. Methyl 2-(6-(4-(dimethylamino)phenoxy)-4-oxo-7-(4-(4-(trifluoromethyl)phenoxy) butanamido)quinazolin-3(4H)-yl)acetate (22m). White powder (54% yield), mp: 134–136 °C. ^{1}H NMR (400 MHz, DMSO-d_6) δ 9.93 (s, 1H), 8.60 (s, 1H), 8.25 (s, 1H), 7.63 (d, *J* = 8.6 Hz, 2H), 7.14 (s, 1H), 7.11 (d, *J* = 8.5 Hz, 2H), 7.03 (d, *J* = 9.0 Hz, 2H), 6.80 (d, *J* = 9.0 Hz, 2H), 4.75 (s, 2H), 4.13 (t, *J* = 6.3 Hz, 2H), 3.67 (s, 3H), 2.92 (s, 6H), 2.75 (t, *J* = 7.2 Hz, 2H), 2.13–2.04 (m, 2H). ^{13}C NMR (101 MHz, DMSO-d_6) δ 172.1, 168.4, 161.4, 159.2, 148.8, 148.2, 146.7, 144.8, 143.6, 134.7, 126.9 (q, *J* = 3.6 Hz), 125.9, 123.2, 121.6, 121.0 (d, *J* = 32.0 Hz), 118.2, 116.2, 114.9, 113.5, 108.7, 99.6, 67.4, 52.3,

47.1, 40.4, 32.8, 24.4. HRMS (ESI): *m/z* (M + H^+) calcd for $C_{30}H_{30}F_3N_4O_6$, 599.2112, found: 599.2116.

4.1.1.6.16. Methyl 2-(6-(3-morpholinophenoxy)-4-oxo-7-(2-((4-(trifluoromethyl)benzyl)oxy) acetamido)quinazolin-3(4H)-yl)acetate (22n). White powder (68% yield), mp: 142−144 °C. ^{1}H NMR (400 MHz, DMSO-d_6) δ 9.67 (s, 1H), 8.66 (s, 1H), 8.30 (s, 1H), 7.61 (d, *J* = 8.6 Hz, 2H), 7.58 (s, 2H), 7.34 (s, 1H), 7.33−7.28 (m, 1H), 6.87 (dd, *J* = 8.3, 2.1 Hz, 1H), 6.82−6.79 (m, 1H), 6.57 (dd, *J* = 8.0, 2.0 Hz, 1H), 4.77 (d, *J* = 11.5 Hz, 4H), 4.33 (d, *J* = 3.4 Hz, 2H), 3.77−3.68 (m, 8H), 3.68 (s, 3H). ^{13}C NMR (101 MHz, DMSO-d_6) δ 168.4 (d, *J* = 13.2 Hz), 159.2, 155.8, 153.0, 147.3, 146.6, 144.4, 142.3, 134.2, 130.6, 128.4, 128.0, 127.9, 127.7, 125.4, 125.0 (q, *J* = 3.7 Hz), 116.8 (d, *J* = 27.5 Hz), 111.4, 110.6, 109.9, 106.5, 71.6, 71.4, 69.7, 65.9, 52.4, 47.9. HRMS (ESI): *m/z* (M + H^+) calcd for $C_{31}H_{30}F_3N_4O_7$, 627.2061, found: 627.2069.

4.1.1.6.17. Methyl 2-(6-(3-morpholinophenoxy)-4-oxo-7-(4-(4-(trifluoromethyl)phenoxy) butanamido)quinazolin-3(4H)-yl)acetate (22O). White powder (60% yield), mp: 178−180 °C. ^{1}H NMR (400 MHz, DMSO-d_6) δ 9.92 (s, 1H), 8.59 (s, 1H), 8.27 (s, 1H), 7.63 (d, *J* = 8.7 Hz, 2H), 7.31 (d, *J* = 8.2 Hz, 1H), 7.27 (s, 1H), 7.10 (d, *J* = 8.7 Hz, 2H), 6.85 (dd, *J* = 8.4, 2.0 Hz, 1H), 6.76 (s, 1H), 6.54 (dd, *J* = 8.0, 1.8 Hz, 1H), 4.77 (s, 2H), 4.12 (t, *J* = 6.3 Hz, 2H), 3.74−3.69 (m, 4H), 3.68 (s, 3H), 3.15−3.10 (m, 4H), 2.72 (t, *J* = 7.2 Hz, 2H), 2.07 (p, *J* = 6.8 Hz, 2H). ^{13}C NMR (101 MHz, DMSO-d_6) δ 172.1, 168.4, 161.4, 159.2, 156.1, 152.9, 147.5, 147.0, 144.1, 135.3, 130.4, 129.6, 126.9 (q, *J* = 3.6 Hz), 121.0 (d, *J* = 32.0 Hz), 118.5, 116.4, 114.9, 111.3, 110.5, 110.3, 106.9, 67.4, 65.9, 52.34, 48.0, 47.1, 32.7, 24.4. HRMS (ESI): *m/z* (M + H^+) calcd for $C_{32}H_{32}F_3N_4O_7$, 641.2218, found: 641.2213.

4.1.1.6.18. N-(6-(3-(dimethylamino)phenoxy)-4-oxo-3,4-dihydroquinazolin-7-yl)-4-(4-(trifluoromethyl)phenoxy)butanamide (22p). Red powder (70% yield), mp > 210 °C. ^{1}H NMR (400 MHz, DMSO-d_6) δ 12.11 (s, 1H), 9.86 (s, 1H), 8.53 (s, 1H), 7.99 (s, 1H), 7.62 (d, *J* = 8.7 Hz, 2H), 7.27 (s, 1H), 7.27−7.21 (m, 1H), 7.10 (d, *J* = 8.6 Hz, 2H), 6.61 (dd, *J* = 8.4, 2.1 Hz, 1H), 6.49 (t, *J* = 2.2 Hz, 1H), 6.36 (dd, *J* = 7.9, 1.8 Hz, 1H), 4.11 (t, *J* = 6.3 Hz, 2H), 2.90 (s, 6H), 2.71 (t, *J* = 7.3 Hz, 2H), 2.08 (dd, *J* = 13.4, 6.7 Hz, 2H). ^{13}C NMR (101 MHz, DMSO-d_6) δ 172.0, 161.4, 159.9, 156.1, 152.1, 147.3, 144.7, 144.4, 134.8, 130.3, 126.9 (q, *J* = 3.8 Hz), 123.2, 121.2, 120.8, 117.8, 114.9, 110.3, 108.9, 107.3, 104.1, 67.4, 40.0, 32.7, 24.4. HRMS (ESI): *m/z* (M + H^+) calcd for $C_{27}H_{26}F_3N_4O_4$, 527.1901, found: 527.1899.

4.1.1.6.19. 2-((4-cyanobenzyl)oxy)-N-(6-(3-(dimethylamino)phenoxy)-4-oxo-3,4-dihydroquinazolin-7-yl)acetamide (22q). Red powder (55% yield), mp > 210 °C. ^{1}H NMR (400 MHz, DMSO-d_6) δ 9.50 (s, 1H), 8.51 (s, 1H), 8.02 (s, 1H), 7.68 (d, *J* = 8.2 Hz, 2H), 7.52 (d, *J* = 8.2 Hz, 2H), 7.34 (s, 1H), 7.25−7.20 (m, 1H), 6.60 (dd, *J* = 8.4, 2.2 Hz, 1H), 6.44 (t, *J* = 2.2 Hz, 1H), 6.31 (dd, *J* = 8.0, 1.9 Hz, 1H), 4.72 (s, 2H), 4.29 (s, 2H), 2.89 (s, 6H). ^{13}C NMR (101 MHz, DMSO-d_6) δ 168.1, 156.5, 152.1, 146.1, 145.1, 143.2, 133.1, 132.2, 130.3, 129.7, 127.9, 118.7, 118.5, 117.2, 116.6, 111.4, 110.3, 108.7, 106.3, 103.2, 71.6, 69.7. HRMS (ESI): *m/z* (M + H^+) calcd for $C_{26}H_{24}N_5O_4$, 470.1823, found: 470.1821.

4.1.1.6.20. 3-Cyano-N-(6-(3-(dimethylamino)phenoxy)-4-oxo-3,4-dihydroquinazolin-7-yl)benzamide (22r). Gray powder (50% yield), mp > 210 °C. ^{1}H NMR (400 MHz, DMSO-d_6) δ 12.21 (s, 1H), 10.30 (s, 1H), 8.28 (d, *J* = 5.8 Hz, 2H), 8.20 (d, *J* = 7.9 Hz, 1H), 8.10−8.03 (m, 2H), 7.76−7.71 (m, 1H), 7.42 (s, 1H), 7.25−7.17 (m, 1H), 6.58 (d, *J* = 8.4 Hz, 1H), 6.50 (s, 1H), 6.37 (d, *J* = 7.8 Hz, 1H), 2.89 (s, 6H). ^{13}C NMR (101 MHz, DMSO-d_6) δ 164.3, 159.9, 156.3, 152.1, 148.8, 144.6, 144.6, 135.3, 135.3, 134.3, 132.7, 131.6, 130.3, 129.8, 121.8, 119.6, 118.2, 111.5, 111.5, 108.7, 106.8, 103.6. HRMS (ESI): *m/z* (M + H^+) calcd for $C_{24}H_{20}N_5O_3$, 426.1561, found: 426.1566.

4.1.1.6.21. N-(6-(3-morpholinophenoxy)-4-oxo-3,4-dihydroquinazolin-7-yl)-2-((4-(trifluoromethyl)benzyl)oxy)acetamide (22s). White powder (60% yield), mp > 210 °C. ^{1}H NMR (400 MHz, DMSO-d_6) δ 12.19 (s, 1H), 9.62 (s, 1H), 8.61 (s, 1H), 8.03 (s, 1H), 7.57 (s, 4H), 7.33 (d, *J* = 2.1 Hz, 1H), 7.30 (d, *J* = 8.2 Hz, 1H), 6.86 (dd, *J* = 8.3, 2.0 Hz, 1H), 6.81−6.78 (m, 1H), 6.55 (dd, *J* = 7.9, 1.9 Hz, 1H), 4.75 (s, 2H), 4.31 (s, 2H), 3.72−3.69 (m, 4H), 3.13−3.08 (m, 4H). ^{13}C NMR (101 MHz, DMSO-d_6) δ 168.4, 159.8, 156.0, 153.0, 146.2, 145.2, 144.8, 142.3 (d, *J* = 1.0 Hz), 133.9, 130.5, 128.2 (d, *J* = 31.6 Hz), 127.8, 125.5, 125.1 (q, *J* = 3.8 Hz), 118.1, 117.0, 111.3, 110.7, 109.8, 106.5, 71.6, 69.7, 65.9, 47.9. HRMS (ESI): *m/z* (M + H^+) calcd for $C_{28}H_{26}F_3N_4O_5$, 555.1850, found: 555.1853.

4.1.1.6.22. N-(6-(3-morpholinophenoxy)-4-oxo-3,4-dihydroquinazolin-7-yl)-4-(4-(trifluoromethyl)phenoxy)butanamide (22t). White powder (88% yield), mp > 210 °C. ^{1}H NMR (400 MHz, DMSO-d_6) δ 12.12 (s, 1H), 9.86 (s, 1H), 8.54 (s, 1H), 8.00 (s, 1H), 7.62 (d, *J* = 8.7 Hz, 2H), 7.30 (d, *J* = 8.2 Hz, 1H), 7.27 (s, 1H), 7.10 (d, *J* = 8.6 Hz, 2H), 6.84 (dd, *J* = 8.3, 2.0 Hz, 1H), 6.76−6.73 (m, 1H), 6.53 (dd, *J* = 7.9, 1.9 Hz, 1H), 4.11 (t, *J* = 6.3 Hz, 2H), 3.73−3.69 (m, 4H), 3.14−3.10 (m, 4H), 2.70 (t, *J* = 7.3 Hz, 2H), 2.07 (dd, *J* = 8.6, 5.0 Hz, 2H). ^{13}C NMR (101 MHz, DMSO-d_6) δ 172.0, 161.4, 159.8, 156.2, 152.9, 147.1, 144.9, 144.4, 135.0, 130.4, 128.1, 127.9, 126.9 (q, *J* = 3.6 Hz), 118.7, 117.8, 114.9, 111.2, 110.5, 110.3, 106.9, 67.4, 66.0, 48.0, 32.7, 24.4. HRMS (ESI): *m/z* (M + H^+) calcd for $C_{29}H_{28}F_3N_4O_5$, 569.2006, found: 569.1993.

4.1.1.7. Synthesis of intermediates 23a and 23b. To a solution of **14a or 22n** (1.0 mmol) in THF (6 mL) and H_2O (3 mL), LiOH (72 mg, 3 mmol) was added. The reaction mixture was stirred at room temperature for 0.5 h and adjusted to neutral (pH = 7) by adding aqueous HCl solution (1 N) to give the white solid **23a-23b** in the yield of 85−90%.

4.1.1.8. Synthesis of compounds 24a-24e. To a solution of **23a or 23b** (1.0 mmol) and DIC (464 μL, 3 equiv.) in THF (30 mL), HOSu (345 mg, 3 equiv.) was added. The reaction mixture was stirred at room temperature overnight. Then amines (5 equiv.) were added. The reaction mixture was continually stirred at room temperature for 3 h and filtered. The filtration was concentrated under reduced pressure, and the residue was purified with flash column chromatography on silica gel to give the compounds **24a-24e** in the yield of 45−90%.

4.1.1.8.1. N-(6-(3-(dimethylamino)phenoxy)-4-oxo-3-(2-oxo-2-(piperidin-1-yl)ethyl)-3,4-dihydroquinazolin-7-yl)-2-((4-(trifluoromethyl)benzyl)oxy)acetamide (24a). Yellow powder (45% yield), mp: 85−86 °C. ^{1}H NMR (400 MHz, DMSO-d_6) δ 9.64 (s, 1H), 8.64 (s, 1H), 8.18 (s, 1H), 7.56 (s, 4H), 7.36 (s, 1H), 7.24 (t, *J* = 8.1 Hz, 1H), 6.63 (d, *J* = 7.4 Hz, 1H), 6.52 (s, 1H), 6.36 (d, *J* = 7.6 Hz, 1H), 4.85 (s, 2H), 4.75 (s, 2H), 4.33 (s, 2H), 3.44 (d, *J* = 24.5 Hz, 4H), 2.89 (s, 6H), 1.59 (s, 4H), 1.44 (s, 2H). ^{13}C NMR (101 MHz, DMSO-d_6) δ 168.4, 164.4, 159.2, 156.0, 152.2, 148.0, 146.3, 144.5, 142.3, 134.0, 130.4, 129.6, 128.0, 127.8, 125.1 (q, *J* = 3.7 Hz), 116.9, 116.8, 110.9, 109.0, 106.5, 103.5, 71.6, 69.7, 46.6, 45.2, 42.6, 39.9, 25.8, 25.1, 23.9. HRMS (ESI): *m/z* (M + H^+) calcd for $C_{33}H_{35}F_3N_5O_5$, 638.2585, found: 638.2580.

4.1.1.8.2. N-(6-(3-(dimethylamino)phenoxy)-3-(2-(4-fluoropiperidin-1-yl)-2-oxoethyl)-4-oxo-3,4-dihydroquinazolin-7-yl)-2-((4-(trifluoromethyl)benzyl)oxy)acetamide (24b). Yellow powder (50% yield), mp: 99−100 °C. ^{1}H NMR (400 MHz, DMSO-d_6) δ 9.65 (s, 1H), 8.65 (s, 1H), 8.18 (s, 1H), 7.56 (s, 4H), 7.36 (s, 1H), 7.24 (t, *J* = 8.1 Hz, 1H), 6.64−6.62 (m, 1H), 6.52 (s, 1H), 6.36 (dd, *J* = 7.8, 1.1 Hz, 1H), 4.90 (d, *J* = 3.8 Hz, 2H), 4.75 (s, 2H), 4.33 (s, 2H), 3.67−3.61 (m, 1H), 3.56−3.43 (m, 4H), 2.89 (s, 6H), 2.03−1.96 (m, 1H), 1.80 (dd, *J* = 17.9, 9.4 Hz, 2H), 1.68−1.56 (m, 1H). ^{13}C NMR (101 MHz, DMSO-d_6) δ 168.4, 164.9, 159.2, 156.0, 152.2, 147.9, 146.4, 144.5, 142.3, 134.0, 130.4, 128.0, 127.8, 125.5, 125.1 (q, *J* = 3.7 Hz), 122.8, 116.9 (d, *J* = 14.0 Hz)., 110.9, 109.0, 106.5, 103.5, 88.9, 71.6, 69.7, 46.5, 40.6, 39.9, 31.2. HRMS (ESI): *m/z* (M + H^+) calcd for $C_{33}H_{34}F_4N_5O_5$, 656.2491, found: 656.2496.

4.1.1.8.3. N-(3-(2-(4,4-difluoropiperidin-1-yl)-2-oxoethyl)-6-(3-(dimethylamino)phenoxy)-4-oxo-3,4-dihydroquinazolin-7-yl)-2-((4-(trifluoromethyl)benzyl)oxy)acetamide (24c). Yellow powder (46% yield), mp: 102–103 °C. ^{1}H NMR (400 MHz, DMSO-d_6) δ 9.65 (s, 1H), 8.65 (s, 1H), 8.18 (s, 1H), 7.56 (s, 4H), 7.37 (s, 1H), 7.24 (s, 1H), 6.64 (s, 1H), 6.52 (s, 1H), 6.37 (s, 1H), 4.94 (s, 2H), 4.75 (s, 2H), 4.32 (s, 2H), 3.60 (d, J = 31.1 Hz, 4H), 2.88 (s, 6H), 2.14–1.92 (m, 4H). ^{13}C NMR (101 MHz, DMSO-d_6) δ 168.4, 165.2, 159.2, 156.0, 152.2, 147.9, 146.4, 144.5, 142.3, 134.1, 130.4, 129.6, 128.3, 128.0, 127.8, 125.1 (q, J = 3.7 Hz), 122.5, 116.9 (d, J = 12.1 Hz), 110.9, 109.0, 106.5, 103.5, 71.6, 69.7, 46.5, 41.2, 39.9, 26.6. HRMS (ESI): m/z (M + H$^+$) calcd for $C_{33}H_{33}F_5N_5O_5$, 674.2396, found: 674.2390.

4.1.1.8.4. N-(3-(2-(3,3-difluoropiperidin-1-yl)-2-oxoethyl)-6-(3-(dimethylamino)phenoxy)-4-oxo-3,4-dihydroquinazolin-7-yl)-2-((4-(trifluoromethyl)benzyl)oxy)acetamide (24d). Yellow powder (62% yield), mp: 106–107 °C. ^{1}H NMR (400 MHz, DMSO-d_6) δ 9.65 (s, 1H), 8.65 (s, 1H), 8.19 (s, 1H), 7.56 (s, 4H), 7.36 (s, 1H), 7.24 (t, J = 8.0 Hz, 1H), 6.63 (d, J = 7.8 Hz, 1H), 6.52 (s, 1H), 6.37 (d, J = 7.5 Hz, 1H), 4.91 (d, J = 20.1 Hz, 2H), 4.75 (s, 2H), 4.33 (s, 2H), 3.91 (t, J = 11.2 Hz, 1H), 3.78 (t, J = 11.9 Hz, 1H), 3.53 (d, J = 32.2 Hz, 2H), 2.89 (s, 6H), 2.12–2.08 (m, 2H), 1.77 (s, 1H), 1.61 (s, 1H). ^{13}C NMR (101 MHz, DMSO-d_6) δ 168.4, 165.6 (br s), 159.2 (d, J = 3.1 Hz), 156.0, 152.2, 147.8 (dd, J = 7.5, 1.1 Hz), 146.4, 144.4, 142.3 (d, J = 1.0 Hz), 134.0, 130.4, 128.3, 128.0, 127.8, 125.5, 125.1 (q, J = 3.7 Hz), 122.8, 116.8 (d, J = 9.5 Hz), 110.9, 109.0, 106.5, 103.5, 71.6, 69.7, 46.6, 46.6, 43.2, 40.8, 39.9, 13.9. HRMS (ESI): m/z (M + H$^+$) calcd for $C_{33}H_{33}F_5N_5O_5$, 674.2396, found: 674.2399.

4.1.1.8.5. N-(3-(2-(3,3-difluoropiperidin-1-yl)-2-oxoethyl)-6-(3-morpholinophenoxy)-4-oxo-3,4-dihydroquinazolin-7-yl)-2-((4-(trifluoromethyl)benzyl)oxy)acetamide (24e). White powder (88% yield), mp > 210 °C. ^{1}H NMR (400 MHz, DMSO-d_6) δ 9.66 (s, 1H), 8.65 (s, 1H), 8.20 (d, J = 2.6 Hz, 1H), 7.57 (s, 4H), 7.34 (d, J = 2.8 Hz, 1H), 7.31 (d, J = 8.2 Hz, 1H), 6.87 (dd, J = 8.4, 2.1 Hz, 1H), 6.81 (d, J = 2.0 Hz, 1H), 6.56 (dd, J = 8.0, 2.0 Hz, 1H), 4.94 (s, 1H), 4.89 (s, 1H), 4.75 (s, 2H), 4.33 (s, 2H), 3.91 (t, J = 11.5 Hz, 1H), 3.76 (d, J = 12.2 Hz, 1H), 3.71–3.68 (m, 4H), 3.59–3.55 (m, 1H), 3.52–3.47 (m, 1H), 3.13–3.10 (m, 4H), 2.09 (dd, J = 13.0, 6.7 Hz, 2H), 1.77 (s, 1H), 1.61 (s, 1H). ^{13}C NMR (101 MHz, DMSO-d_6) δ 168.5, 165.7, 159.2, 156.0, 153.0, 147.9, 147.9, 146.4, 144.5, 142.3, 134.1, 130.6, 128.3, 128.0, 127.9, 125.5, 125.1 (q, J = 3.7 Hz), 116.9 (d, J = 1.4 Hz), 111.4, 110.9, 109.8, 106.4, 71.6, 69.7, 65.9, 47.9, 46.6, 43.2, 40.9, 29.1, 22.4. HRMS (ESI): m/z (M + H$^+$) calcd for $C_{35}H_{35}F_5N_5O_6$, 716.2502, found: 716.2499.

4.1.2. General procedure for the synthesis of compounds 30a-30j, 34a-34f, 35, 36a, 36b

4.1.2.1. Synthesis of intermediate 26. The mixture of dimethyl 2-aminoterephthalate **25** (2.1 g, 10 mmol) and *N*-iodosuccinimide (2.5 g, 11 mmol) in acetic acid (200 mL) was stirred at room temperature for 24 h, and water (30 mL) was then added. The reaction mixture was adjusted to neutral (pH = 7) by adding saturated sodium bicarbonate solution, and extracted with ethyl acetate. The organic phase was washed with brine and dried over $MgSO_4$. Solvent was removed under reduced pressure, and the residue was purified with flash column chromatography on silica gel to give dimethyl 2-amino-5-iodoterephthalate (**26**) in the yield of 57%.

4.1.2.2. Synthesis of intermediates 27a-27c. To a solution of **26** (3.4 g, 10 mmol) and phenylboronic acid derivatives (20 mmol, 2 equiv.) in 1, 4-dioxane and H_2O (1, 4-dioxane/H_2O = 2:1), $Pd(PPh_3)_4$ (1.3 g, 1.1 mmol) and Na_2CO_3 (5.3 g, 50 mmol) were added. The reaction mixture was heated to 100 °C and stirred overnight under N_2 atmosphere. Then the mixture was filtered and the filtrate was concentrated under reduced pressure. The reaction residue was dissolved in DCM, and washed with water. The aqueous phase was extracted with DCM, and the organic phase was combined and washed with brine and dried over anhydrous $MgSO_4$. Solvent was removed, and the residue was purified with flash column chromatography on silica gel to give intermediates **27a-27c** in the yield of 80–90%.

4.1.2.3. Synthesis of intermediates 28a-28c. To a solution of **27a-27c** (1.0 mmol) in THF (6 mL) and H_2O (3 mL), LiOH (72.0 mg, 3 mmol) was added. The reaction mixture was stirred at room temperature for 0.5 h and adjusted to acidity (pH = 2) by adding aqueous HCl solution (6 N) to give the yellow solid **28a-28c** in the yield of 80–90%.

4.1.2.4. Synthesis of intermediates 29a-29c. The mixture of **28a-28c** (1.0 mmol) in formamide (10 mL) was heated to 160 °C, and stirred for 5 h. Then the reaction mixture was concentrated under reduced pressure, and the residue was purified with flash column chromatography on silica gel to give the intermediates **29a-29c** in the yield of 50–60%.

4.1.2.5. Synthesis of compounds 30a-30j. To a mixture of **29a-29c** (0.1 mmol) in THF (10 mL), amines (0.2 mmol) and HATU (114.0 mg, 3.0 mmol) were added. The reaction mixture was stirred at room temperature overnight and concentrated under reduced pressure. The residue was purified with flash column chromatography on silica gel to give the compounds **30a-30j** in the yield of 70%–90%.

4.1.2.5.1. 6-(3-chlorophenyl)-4-oxo-N-(2-((4-(trifluoromethyl)benzyl)oxy)ethyl)-3,4-dihydroquinazoline-7-carboxamide (30a). White powder (75% yield), mp: 177–179 °C. ^{1}H NMR (400 MHz, DMSO-d_6) δ 12.47 (s, 1H), 8.78–8.74 (m, 1H), 8.19 (s, 1H), 8.05 (s, 1H), 7.71 (d, J = 8.0 Hz, 2H), 7.67 (s, 1H), 7.55 (d, J = 8.0 Hz, 2H), 7.47 (d, J = 1.5 Hz, 1H), 7.40 (q, J = 4.4 Hz, 3H), 4.56 (s, 2H), 3.45 (t, J = 5.7 Hz, 2H), 3.40–3.37 (m, 2H). ^{13}C NMR (101 MHz, DMSO-d_6) δ 167.9, 160.4, 148.0, 146.6, 143.4, 142.5, 141.2, 135.9, 133.0, 130.2, 128.1, 128.0, 127.8, 127.5, 127.1, 127.0, 126.4, 125.7, 125.1 (q, J = 3.6 Hz), 123.0, 71.0, 68.3. HRMS (ESI): m/z (M + H$^+$) calcd for $C_{25}H_{20}ClF_3N_3O_3$, 502.1140, found: 502.1149.

4.1.2.5.2. 6-(3-chlorophenyl)-N-(3-(4-chlorophenyl)propyl)-4-oxo-3,4-dihydroquinazoline-7-carboxamide (30b). White powder (80% yield), mp: 140–142 °C. ^{1}H NMR (400 MHz, DMSO-d_6) δ 12.45 (s, 1H), 8.61–8.56 (m, 1H), 8.19 (s, 1H), 8.06 (s, 1H), 7.67 (s, 1H), 7.49 (s, 1H), 7.45–7.41 (m, 3H), 7.33 (d, J = 8.3 Hz, 2H), 7.18 (d, J = 8.3 Hz, 2H), 3.12 (q, J = 6.7 Hz, 2H), 2.47–2.43 (m, 2H), 1.63 (dd, J = 14.6, 7.3 Hz, 2H). ^{13}C NMR (101 MHz, DMSO-d_6) δ 167.6, 160.3, 148.0, 146.5, 142.9, 141.2, 140.6, 135.9, 133.0, 130.4, 130.3, 130.2, 128.2, 128.1, 127.6, 127.2, 126.9, 126.3, 122.9, 38.4, 31.6, 30.3. HRMS (ESI): m/z (M + H$^+$) calcd for $C_{24}H_{20}Cl_2N_3O_2$, 452.0927, found: 452.0928.

4.1.2.5.3. 6-(3-chlorophenyl)-4-oxo-N-(3-phenylpropyl)-3,4-dihydroquinazoline-7-carboxamide (30c). White powder (78% yield), mp: 99–100 °C. ^{1}H NMR (400 MHz, DMSO-d_6) δ 12.45 (s, 1H), 8.62–8.58 (m, 1H), 8.19 (s, 1H), 8.06 (s, 1H), 7.67 (s, 1H), 7.49 (s, 1H), 7.43 (q, J = 4.3 Hz, 3H), 7.30–7.25 (m, 2H), 7.19–7.14 (m, 3H), 3.14 (d, J = 6.1 Hz, 2H), 2.46 (d, J = 7.8 Hz, 2H), 1.69–1.63 (m, 2H). ^{13}C NMR (101 MHz, DMSO-d_6) δ 167.6, 160.2, 148.0, 146.5, 142.9, 141.6, 141.2, 135.9, 133.0, 130.2, 128.3, 128.2, 128.1, 127.6, 127.2, 126.9, 126.3, 125.7, 122.8, 38.5, 32.4, 30.4. HRMS (ESI): m/z (M + H$^+$) calcd for $C_{24}H_{21}ClN_3O_2$, 418.1317, found: 418.1307.

4.1.2.5.4. 6-(3-chlorophenyl)-4-oxo-N-(3-(4-(trifluoromethyl)phenoxy)propyl)-3,4-dihydroquinazoline-7-carboxamide (30d). White powder (86% yield), mp: 90–91 °C. ^{1}H NMR (400 MHz, DMSO-d_6) δ 8.66–8.63 (m, 1H), 8.19 (s, 1H), 8.06 (s, 1H), 7.69 (s, 1H), 7.64 (d, J = 8.4 Hz, 2H), 7.48 (s, 1H), 7.42 (dd, J = 6.0, 3.3 Hz, 2H), 7.39 (dd, J = 5.6, 2.7 Hz, 1H), 7.36–7.23 (m, 1H), 7.04 (d, J = 8.8 Hz, 2H), 3.89 (t, J = 6.1 Hz, 2H), 3.27 (dd, J = 12.6, 6.2 Hz, 2H), 1.87–1.79 (m, 2H). ^{13}C NMR (101 MHz, DMSO-d_6) δ 167.7, 161.4, 160.3, 148.0, 146.6, 142.7, 141.2, 135.8, 133.0, 130.2, 128.7, 128.1, 127.5, 127.1, 127.0, 126.9

(d, J = 4.4 Hz), 126.2, 122.9, 121.0 (d, J = 31.8 Hz), 114.9, 65.4, 35.7, 28.3. HRMS (ESI): m/z ($M + H^+$) calcd for $C_{25}H_{20}ClF_3N_3O_3$, 502.1140, found: 502.1143.

4.1.2.5.5. 6-(3-fluorophenyl)-4-oxo-N-(2-((4-(trifluoromethyl) benzyl)oxy)ethyl)-3,4-dihydroquinazoline-7-carboxamide (30e). White powder (80% yield), mp: 176–178 °C. ^{1}H NMR (400 MHz, DMSO-d_6) δ 12.46 (s, 1H), 8.78–8.74 (m, 1H), 8.19 (s, 1H), 8.06 (s, 1H), 7.71 (d, J = 7.9 Hz, 2H), 7.67 (s, 1H), 7.55 (d, J = 7.9 Hz, 2H), 7.40 (dd, J = 14.5, 7.4 Hz, 1H), 7.30–7.25 (m, 2H), 7.21–7.15 (m, 1H), 4.55 (s, 2H), 3.45 (d, J = 5.1 Hz, 2H), 3.38 (d, J = 5.2 Hz, 2H). ^{13}C NMR (101 MHz, DMSO-d_6) δ 167.9, 163.2, 160.8, 160.4, 147.9, 146.6, 143.4, 142.6, 141.5 (d, J = 8.0 Hz), 136.1 (d, J = 1.9 Hz), 130.3 (d, J = 8.4 Hz), 127.8, 127.0, 126.4, 125.7, 125.1 (q, J = 3.5 Hz), 124.6 (d, J = 2.4 Hz), 123.0 (d, J = 7.7 Hz), 115.1 (d, J = 22.2 Hz), 114.4 (d, J = 20.9 Hz), 71.0, 68.3, 38.9. HRMS (ESI): m/z ($M + H^+$) calcd for $C_{25}H_{20}F_4N_3O_3$, 486.1435, found: 486.1431.

4.1.2.5.6. N-(3-(4-chlorophenyl)propyl)-6-(3-fluorophenyl)-4-oxo-3,4-dihydroquinazoline-7-carboxamide (30f). White powder (70% yield), mp: 165–167 °C. ^{1}H NMR (400 MHz, DMSO-d_6) δ 12.45 (s, 1H), 8.59–8.54 (m, 1H), 8.19 (s, 1H), 8.06 (s, 1H), 7.67 (s, 1H), 7.45 (dd, J = 11.0, 4.8 Hz, 1H), 7.33 (s, 1H), 7.31 (d, J = 3.4 Hz, 2H), 7.29 (d, J = 1.6 Hz, 1H), 7.21–7.18 (m, 2H), 7.17 (s, 1H), 3.15–3.10 (m, 2H), 2.48–2.43 (m, 2H), 1.65–1.59 (m, 2H). ^{13}C NMR (101 MHz, DMSO-d_6) δ 167.6, 163.1, 160.7, 160.2, 147.9, 146.4, 142.9, 141.5 (d, J = 8.0 Hz), 140.6, 136.1 (d, J = 1.9 Hz), 130.3 (d, J = 7.9 Hz), 130.2, 128.1, 126.9, 126.3, 124.6 (d, J = 2.6 Hz), 122.8, 115.2 (d, J = 22.2 Hz), 114.4 (d, J = 21.0 Hz), 38.3, 31.6, 30.2. HRMS (ESI): m/z ($M + H^+$) calcd for $C_{24}H_{20}ClFN_3O_2$, 436.1223, found: 436.1220.

4.1.2.5.7. 6-(3-fluorophenyl)-4-oxo-N-(3-phenylpropyl)-3,4-dihydroquinazoline-7-carboxamide (30g). White powder (80% yield), mp: 116–118 °C. ^{1}H NMR (400 MHz, DMSO-d_6) δ 12.45 (s, 1H), 8.60–8.56 (m, 1H), 8.19 (s, 1H), 8.07 (s, 1H), 7.67 (s, 1H), 7.45 (dd, J = 14.3, 8.0 Hz, 1H), 7.32–7.29 (m, 2H), 7.28–7.25 (m, 2H), 7.23–7.19 (m, 1H), 7.16 (dd, J = 5.9, 4.7 Hz, 3H), 3.16–3.10 (m, 2H), 2.46 (d, J = 7.8 Hz, 2H), 1.64 (dd, J = 14.6, 7.3 Hz, 2H). ^{13}C NMR (101 MHz, DMSO-d_6) δ 167.6, 163.1, 160.7, 160.3, 147.9, 146.5, 142.9, 141.6, 141.5 (d, J = 8.1 Hz), 136.1 (d, J = 2.0 Hz), 130.3 (d, J = 8.5 Hz), 128.3 (d, J = 2.9 Hz), 126.9, 126.3, 125.7, 124.6 (d, J = 2.6 Hz), 122.8, 115.2 (d, J = 22.2 Hz), 114.4 (d, J = 20.9 Hz), 38.5, 32.4, 30.4. HRMS (ESI): m/z ($M + H^+$) calcd for $C_{24}H_{21}FN_3O_2$, 402.1612, found: 402.1602.

4.1.2.5.8. 4-Oxo-N-(2-((4-(trifluoromethyl)benzyl)oxy)ethyl)-6-(3-(trifluoromethyl)phenyl)-3,4-dihydroquinazoline-7-carboxamide (30 h). White powder (90% yield), mp: 201–203 °C. ^{1}H NMR (400 MHz, DMSO-d_6) δ 12.50 (br s, 1H), 8.82–8.77 (m, 1H), 8.21 (s, 1H), 8.09 (s, 1H), 7.73 (dd, J = 17.1, 9.1 Hz, 6H), 7.63–7.58 (m, 1H), 7.54 (d, J = 8.0 Hz, 2H), 4.53 (s, 2H), 3.43 (t, J = 5.6 Hz, 2H), 3.38–3.32 (m, 2H). ^{13}C NMR (101 MHz, DMSO-d_6) δ 167.8, 160.4, 148.1, 146.8, 143.3, 142.4, 140.1, 135.7, 132.4, 129.5, 129.5, 129.1 (d, J = 31.6 Hz), 128.1, 127.8, 127.1, 126.4, 125.5, 125.1 (q, J = 3.9 Hz), 124.7 (d, J = 4.0 Hz), 123.0, 122.8, 70.9, 68.2, 40.1. HRMS (ESI): m/z ($M + H^+$) calcd for $C_{26}H_{20}F_6N_3O_3$, 536.1403, found: 536.1407.

4.1.2.5.9. N-(3-(4-chlorophenyl)propyl)-4-oxo-6-(3-(trifluoromethyl)phenyl)-3,4-dihydroquinazoline-7-carboxamide (30i). White powder (86% yield), mp: 186–188 °C. ^{1}H NMR (400 MHz, DMSO-d_6) δ 12.50 (s, 1H), 8.67–8.62 (m, 1H), 8.21 (d, J = 2.2 Hz, 1H), 8.10 (s, 1H), 7.81–7.74 (m, 3H), 7.72 (d, J = 7.4 Hz, 2H), 7.69–7.64 (m, 1H), 7.32 (d, J = 8.2 Hz, 2H), 7.15 (d, J = 8.0 Hz, 2H), 3.10 (dd, J = 12.3, 6.2 Hz, 2H), 2.42 (t, J = 7.6 Hz, 2H), 1.59 (dd, J = 14.2, 7.0 Hz, 2H). ^{13}C NMR (101 MHz, DMSO-d_6) δ 167.6, 160.3, 148.1, 146.6, 142.8, 140.6, 140.2, 135.9, 132.6, 130.3 (d, J = 19.0 Hz), 129.6, 129.1 (d, J = 31.5 Hz), 128.2, 127.1, 126.4, 125.5, 124.8 (q, J = 3.7 Hz), 124.4 (d, J = 2.9 Hz), 123.0, 122.8, 38.4, 31.6, 30.2. HRMS (ESI): m/z ($M + H^+$) calcd for $C_{25}H_{20}ClF_3N_3O_2$, 486.1191, found: 486.1199.

4.1.2.5.10. 4-Oxo-N-(3-phenylpropyl)-6-(3-(trifluoromethyl) phenyl)-3,4-dihydroquinazoline-7-carboxamide (30j). White powder (85% yield), mp: 188–190 °C. ^{1}H NMR (400 MHz, DMSO-d_6) δ 12.50 (s, 1H), 8.67–8.62 (m, 1H), 8.21 (s, 1H), 8.10 (s, 1H), 7.77 (d, J = 11.3 Hz, 2H), 7.71 (d, J = 8.2 Hz, 2H), 7.66 (t, J = 7.5 Hz, 1H), 7.26 (t, J = 7.3 Hz, 2H), 7.17 (d, J = 7.1 Hz, 1H), 7.13 (d, J = 7.6 Hz, 2H), 3.11 (dd, J = 12.4, 6.3 Hz, 2H), 2.44 (t, J = 7.6 Hz, 2H), 1.67–1.57 (m, 2H). ^{13}C NMR (101 MHz, DMSO-d_6) δ 167.6, 160.3, 148.1, 146.6, 142.9, 141.6, 140.2, 135.9, 132.6, 129.6, 129.1 (d, J = 31.6 Hz), 128.3 (d, J = 2.9 Hz), 127.1, 126.4, 125.8, 125.5, 124.8 (q, J = 3.8 Hz), 124.4 (d, J = 2.9 Hz), 122.9, 122.8, 38.6, 32.4, 30.3. HRMS (ESI): m/z ($M + H^+$) calcd for $C_{25}H_{21}F_3N_3O_2$, 452.1580, found: 452.1585.

4.1.2.6. Synthesis of intermediates 31-33. To a mixture of **28a-28b** (0.3 mmol) in THF (10 mL), triphosgene (29.7 mg, 0.1 mmol) was added under N_2 atmosphere. The reaction mixture was heated to 50 °C and stirred for 4 h, then concentrated under reduced pressure to give intermediate **31**. To a mixture of **31** in water, glycine methyl ester hydrochloride (113.0 mg, 0.9 mmol) and triethylamine (125.0 μL, 0.9 mmol) was added. The reaction mixture was stirred at room temperature for 6 h and concentrated under reduced pressure to give intermediate **32**. The mixture of **32** in HCOOH was then heated to 110 °C and stirred for 5 h. The reaction mixture was concentrated under reduced pressure and the residue was purified with flash column chromatography on silica gel to give the intermediates **33a-33b** in the yield of 50–65%.

4.1.2.7. Synthesis of compounds 34a-34f. To a mixture of **33a-33b** (0.1 mmol) in THF (10 mL), amine derivatives (0.2 mmol) and HATU (114 mg, 3.0 mmol) were added. The reaction mixture was stirred at room temperature overnight and concentrated under reduced pressure, the residue was purified with flash column chromatography on silica gel to give the compounds **34a-34f** in the yield of 80–95%.

4.1.2.7.1. Methyl 2-(6-(3-fluorophenyl)-4-oxo-7-((2-((4-(trifluoromethyl)benzyl) oxy)ethyl) carbamoyl)quinazolin-3(4H)-yl)acetate (34a). White powder (89% yield), mp > 210 °C. ^{1}H NMR (400 MHz, DMSO-d_6) δ 8.80–8.75 (m, 1H), 8.47 (s, 1H), 8.08 (s, 1H), 7.73 (s, 1H), 7.71 (s, 2H), 7.56 (d, J = 7.7 Hz, 2H), 7.41 (d, J = 6.7 Hz, 1H), 7.29 (d, J = 7.9 Hz, 2H), 7.22–7.17 (m, 1H), 4.89 (s, 2H), 4.56 (s, 2H), 3.72 (s, 3H), 3.49–3.40 (m, 4H). ^{13}C NMR (101 MHz, DMSO-d_6) δ 168.4, 167.7, 159.7, 158.6, 149.0, 147.1, 145.1, 143.4 (d, J = 2.4 Hz), 143.0, 141.3, 136.7, 136.7, 128.1, 127.9, 127.1, 126.5, 125.1 (q, J = 3.9 Hz), 124.6 (d, J = 2.4 Hz), 121.5, 115.1, 114.5, 71.0, 68.3, 52.6, 47.3, 32.4. HRMS (ESI): m/z ($M + H^+$) calcd for $C_{28}H_{24}F_4N_3O_5$, 558.1647, found: 558.1646.

4.1.2.7.2. Methyl 2-(7-((3-(4-chlorophenyl)propyl)carbamoyl)-6-(3-fluorophenyl)-4-oxo quinazolin-3(4H)-yl)acetate (34b). White powder (94% yield), mp: 160–162 °C. ^{1}H NMR (400 MHz, DMSO-d_6) δ 8.60 (d, J = 4.8 Hz, 1H), 8.47 (s, 1H), 8.09 (s, 1H), 7.73 (s, 1H), 7.46 (dd, J = 14.5, 7.7 Hz, 1H), 7.31 (dd, J = 16.3, 7.9 Hz, 4H), 7.22 (d, J = 8.7 Hz, 1H), 7.18 (d, J = 8.1 Hz, 2H), 4.89 (s, 2H), 3.72 (s, 3H), 3.13 (dd, J = 12.0, 6.0 Hz, 2H), 2.45 (t, J = 7.5 Hz, 2H), 1.63 (dd, J = 13.9, 6.9 Hz, 2H). ^{13}C NMR (101 MHz, DMSO-d_6) δ 168.4, 167.5, 163.1, 160.7, 159.7, 149.0, 147.1, 143.3, 141.3 (d, J = 8.1 Hz), 140.6, 136.7 (d, J = 2.2 Hz), 130.4 (d, J = 5.3 Hz), 130.2, 128.2, 127.1, 126.4, 124.7 (d, J = 2.8 Hz), 121.4, 115.3 (d, J = 22.3 Hz), 114.6 (d, J = 21.0 Hz), 52.5, 47.3, 38.4, 31.6, 30.2. HRMS (ESI): m/z ($M + H^+$) calcd for $C_{27}H_{24}ClFN_3O_4$, 508.1434, found: 508.1433.

4.1.2.7.3. Methyl 2-(6-(3-fluorophenyl)-4-oxo-7-((3-phenylpropyl)carbamoyl)quinazolin- 3(4H)-yl)acetate (34c). White powder (92% yield), mp: 120–121 °C. ^{1}H NMR (400 MHz, DMSO-d_6) δ 8.61 (s, 1H), 8.47 (s, 1H), 8.09 (s, 1H), 7.72 (s, 1H), 7.46 (dd, J = 14.5, 7.6 Hz, 1H), 7.29 (dd, J = 14.9, 7.3 Hz, 4H), 7.18 (dd, J = 18.7, 8.0 Hz, 4H), 4.89 (s, 2H), 3.72 (s, 3H), 3.14 (dd, J = 12.4,

6.3 Hz, 2H), 2.46 (d, J = 7.8 Hz, 2H), 1.70–1.60 (m, 2H). ^{13}C NMR (101 MHz, DMSO-d_6) δ 168.4, 167.5, 163.1, 160.7, 159.7, 149.0, 147.1, 143.3, 141.6, 141.3 (d, J = 8.0 Hz), 136.8 (d, J = 1.7 Hz), 130.4 (d, J = 8.8 Hz), 128.3 (d, J = 2.7 Hz), 127.1, 126.4, 125.8, 124.7 (d, J = 2.5 Hz), 121.4, 115.3 (d, J = 22.3 Hz), 114.6 (d, J = 20.4 Hz), 52.5, 47.3, 38.5, 32.4, 30.4. HRMS (ESI): m/z (M + H^+) calcd for $C_{27}H_{25}FN_3O_4$, 474.1824, found: 474.1823.

4.1.2.7.4. Methyl 2-(6-(3-chlorophenyl)-4-oxo-7-((2-((4-(trifluoromethyl)benzyl) oxy)ethyl) carbamoyl)quinazolin-3(4H)-yl)acetate (34d). White powder (80% yield), mp: 169–171 °C. ^{1}H NMR (400 MHz, DMSO-d_6) δ 8.80–8.76 (m, 1H), 8.47 (s, 1H), 8.08 (s, 1H), 7.72 (s, 2H), 7.71 (s, 1H), 7.56 (d, J = 8.0 Hz, 2H), 7.49 (s, 1H), 7.44–7.39 (m, 3H), 4.89 (s, 2H), 4.56 (s, 2H), 3.72 (s, 3H), 3.45 (t, J = 5.4 Hz, 2H), 3.42–3.37 (m, 2H). ^{13}C NMR (101 MHz, DMSO-d_6) δ 168.4, 167.7, 159.7, 149.0, 147.1, 143.3, 142.9, 141.0, 136.5, 133.0, 130.2, 128.1, 128.1, 127.8, 127.7, 127.2 (d, J = 3.7 Hz), 126.5, 125.7, 125.1 (q, J = 3.6 Hz), 123.0, 121.5, 71.0, 68.3, 52.5, 47.3. HRMS (ESI): m/z (M + H^+) calcd for $C_{28}H_{24}ClF_3N_3O_5$, 574.1351, found: 574.1346.

4.1.2.7.5. Methyl 2-(6-(3-chlorophenyl)-7-((3-(4-chlorophenyl) propyl)carbamoyl)-4- oxoquinazolin-3(4H)-yl)acetate (34e). White powder (83% yield), mp: 175–177 °C. ^{1}H NMR (400 MHz, DMSO-d_6) δ 8.62–8.58 (m, 1H), 8.47 (s, 1H), 8.08 (s, 1H), 7.73 (s, 1H), 7.50 (s, 1H), 7.46–7.41 (m, 3H), 7.33 (d, J = 8.3 Hz, 2H), 7.18 (d, J = 8.3 Hz, 2H), 4.89 (s, 2H), 3.72 (s, 3H), 3.13 (dd, J = 12.6, 6.5 Hz, 2H), 2.45 (t, J = 7.6 Hz, 2H), 1.68–1.60 (m, 2H). ^{13}C NMR (101 MHz, DMSO-d_6) δ 168.3, 167.4, 159.6, 149.0, 147.1, 143.2, 141.0, 140.6, 136.5, 133.0, 130.3, 130.2, 130.2, 128.1, 128.1, 127.7, 127.2, 127.1, 126.4, 121.4, 52.5, 47.3, 38.4, 31.6, 30.2. HRMS (ESI): m/z (M + H^+) calcd for $C_{27}H_{24}Cl_2N_3O_4$, 524.1138, found: 524.1136.

4.1.2.7.6. Methyl 2-(6-(3-chlorophenyl)-4-oxo-7-((3-(4-(trifluoromethyl)phenoxy) propyl) carbamoyl)quinazolin-3(4H)-yl)acetate (34f). White powder (88% yield), mp: 190–192 °C. ^{1}H NMR (400 MHz, DMSO-d_6) δ 8.70–8.65 (m, 1H), 8.46 (s, 1H), 8.08 (s, 1H), 7.74 (s, 1H), 7.65 (d, J = 8.7 Hz, 2H), 7.50 (s, 1H), 7.47–7.38 (m, 3H), 7.05 (d, J = 8.6 Hz, 2H), 4.89 (s, 2H), 3.89 (t, J = 6.1 Hz, 2H), 3.72 (s, 3H), 3.33–3.28 (m, 2H), 1.87–1.79 (m, 2H). ^{13}C NMR (101 MHz, DMSO-d_6) δ 168.3, 167.5, 161.4, 159.6, 149.0, 147.1, 143.1, 141.0, 136.5, 133.0, 130.2, 128.7, 128.1, 127.7, 127.2, 127.1, 126.9 (q, J = 3.7 Hz), 126.4, 121.5, 121.0 (d, J = 32.1 Hz), 114.9, 65.4, 52.5, 47.3, 35.7, 28.3. HRMS (ESI): m/z (M + H^+) calcd for $C_{28}H_{24}ClF_3N_3O_5$, 574.1351, found: 574.1341.

4.1.2.8. Synthesis of compound 35. To a mixture of **34f** (573 mg, 1.0 mmol) in THF (6 mL) and H_2O (3 mL), LiOH (72 mg, 3.0 mmol) was added. The reaction mixture was stirred at room temperature for 0.5 h and adjusted to neutral (pH = 7) by adding aqueous HCl solution (1 N) to give the white solid **35** in the yield of 85%.

4.1.2.8.1. 2-(6-(3-chlorophenyl)-4-oxo-7-((3-(4-(trifluoromethyl) phenoxy)propyl)carbamoyl) quinazolin-3(4H)-yl)acetic acid (35). White powder (85% yield), mp: 198–200 °C. ^{1}H NMR (400 MHz, DMSO-d_6) δ 8.67–8.64 (m, 1H), 8.45 (s, 1H), 8.08 (s, 1H), 7.73 (s, 1H), 7.65 (d, J = 8.7 Hz, 2H), 7.50 (s, 1H), 7.43 (dd, J = 5.9, 3.0 Hz, 2H), 7.40 (dd, J = 4.6, 1.9 Hz, 1H), 7.05 (d, J = 8.7 Hz, 2H), 4.76 (s, 2H), 3.89 (t, J = 6.1 Hz, 2H), 3.29–3.20 (m, 2H), 1.83 (dd, J = 12.6, 6.3 Hz, 2H). ^{13}C NMR (101 MHz, DMSO-d_6) δ 169.2, 167.6, 161.4, 159.7, 149.2, 147.2, 142.9, 141.1, 136.3, 133.0, 130.2, 128.1, 127.6, 127.2, 127.1, 126.9 (q, J = 3.7 Hz), 126.3, 125.9, 121.6, 121.0 (d, J = 32.0 Hz), 114.9, 65.4, 47.4, 35.8, 28.3. HRMS (ESI): m/z (M + H^+) calcd for $C_{27}H_{22}ClF_3N_3O_5$, 560.1195, found: 560.1192.

4.1.2.9. Synthesis of compounds 36a and 36b. To a solution of **35** (1.0 mmol) and DIC (464 μL, 3 equiv.) in THF (30 mL), HOSu (345 mg, 3 equiv.) was added, and the reaction mixture was stirred at room temperature overnight. Then amine (5 equiv.) was added, and the mixture was continually stirred at room temperature for 3 h. Solvent was removed under reduced pressure, and the residue was purified with flash column chromatography on silica gel to give **36a** and **36b** in the yield of 80–86%.

4.1.2.9.1. 6-(3-chlorophenyl)-4-oxo-3-(2-oxo-2-(piperidin-1-yl) ethyl)-N-(3-(4-(trifluoromethyl)phenoxy)propyl)-3,4-dihydroquinazoline-7-carboxamide (36a). White powder (86% yield), mp: 153–155 °C. ^{1}H NMR (400 MHz, DMSO-d_6) δ 8.68–8.64 (m, 1H), 8.40 (d, J = 49.8 Hz, 1H), 8.07 (d, J = 8.1 Hz, 1H), 7.73 (d, J = 8.7 Hz, 1H), 7.65 (d, J = 8.7 Hz, 2H), 7.51–7.48 (m, 1H), 7.44–7.42 (m, 2H), 7.41–7.36 (m, 1H), 7.05 (d, J = 8.7 Hz, 2H), 4.92 (d, J = 27.1 Hz, 2H), 3.89 (t, J = 6.1 Hz, 2H), 3.72 (s, 2H), 3.46 (dd, J = 18.5, 13.5 Hz, 4H), 3.31 (q, J = 6.3 Hz, 2H), 1.87–1.81 (m, 2H), 1.54 (d, J = 62.5 Hz, 4H). ^{13}C NMR (101 MHz, DMSO-d_6) δ 168.3, 167.6 (d, J = 9.6 Hz), 164.3, 161.4, 159.7 (d, J = 4.6 Hz), 149.0, 147.2 (d, J = 12.2 Hz), 142.9 (d, J = 28.0 Hz), 141.1 (d, J = 14.3 Hz), 136.3 (d, J = 31.5 Hz), 133.0, 130.2, 128.1, 127.6 (d, J = 7.0 Hz), 127.1 (d, J = 11.4 Hz), 126.9 (q, J = 3.7 Hz), 126.3 (d, J = 12.9 Hz), 123.3, 121.6 (d, J = 21.0 Hz), 121.0 (d, J = 32.1 Hz), 114.9, 65.4, 52.5, 47.3, 35.8, 28.3, 25.2, 23.9. HRMS (ESI): m/z (M + H^+) calcd for $C_{32}H_{31}ClF_3N_4O_4$, 627.1980, found: 627.1982.

4.1.2.9.2. 6-(3-chlorophenyl)-3-(2-(3,3-difluoropiperidin-1-yl)-2-oxoethyl)-4-oxo-N-(3-(4-(trifluoromethyl)phenoxy)propyl)-3,4-dihydroquinazoline-7-carboxamide (36b). White powder (80% yield), mp: 90–91 °C. ^{1}H NMR (400 MHz, DMSO-d_6) δ 8.68–8.64 (m, 1H), 8.35 (d, J = 5.4 Hz, 1H), 8.06 (s, 1H), 7.73 (s, 1H), 7.65 (d, J = 8.7 Hz, 2H), 7.49 (s, 1H), 7.45 (dd, J = 9.6, 5.1 Hz, 1H), 7.42–7.38 (m, 2H), 7.05 (d, J = 8.6 Hz, 2H), 5.01 (d, J = 21.1 Hz, 2H), 3.99–3.77 (m, 4H), 3.63–3.58 (m, 1H), 3.53 (dd, J = 6.9, 2.7 Hz, 1H), 3.32–3.24 (m, 2H), 2.20–2.03 (m, 2H), 1.83 (dd, J = 11.8, 5.5 Hz, 3H), 1.67–1.56 (m, 1H). ^{13}C NMR (101 MHz, DMSO-d_6) δ 167.6, 165.5, 161.40 (d, J = 1.1 Hz), 159.7, 149.5, 147.2, 142.9, 141.1, 136.3, 133.0, 130.2, 128.1, 127.6, 127.2, 127.1, 126.9 (q, J = 3.7 Hz), 126.3, 126.0, 123.3, 121.6, 121.2, 114.9, 65.4, 46.8, 43.3, 40.9, 35.7, 31.7, 28.3, 22.4. HRMS (ESI): m/z (M + H^+) calcd for $C_{32}H_{29}ClF_5N_4O_4$, 663.1792, found: 663.1791.

4.2. Biology

4.2.1. Animals

Male C57BL/6 mice (6–8 weeks old) were purchased from Vital River Experimental Animal Co., Ltd. (Beijing, China). Mice were housed in the specific pathogen-free conditions with a 12 h light/dark cycle and free access to food and water in the animal research center laboratory of Tsinghua University. All animal protocols were conducted in compliance with the Institute of Animal Care and Use Committee (IACUC) of Tsinghua University approved by institutional and national guidelines.

4.2.2. Cell culture

HEK-Blue hNOD1 cells, HEK-Blue hNOD2 cells were purchased from InvivoGen (San Diego, CA) and cultured in Dulbecco's modified Eagle medium (DMEM) (Life Technologies, CA, USA) with 4.5 g/l glucose (Life Technologies), 10% (v/v) fetal bovine serum (FBS) (Gibco, Australia), 1% (v/v) penicillin/streptomycin (Life Technologies), 100 μg/mL Normocin (InvivoGen, San Diego, CA), and additional selective antibiotics according to the manufacturer's protocol. B16F10 cell line was purchased from ATCC (Mannassas, VA, USA) and cultured in DMEM, human monocytic leukemia THP1 cell line was kindly provided by Dr. Wanli Liu (Tsinghua University, Beijing, China) maintained in RPMI-1640 medium (Life Technologies), supplemented with 10% (v/v) FBS, 1% (v/v) penicillin/streptomycin. All the cells were grown at 37 °C in a 5% CO_2 humidified incubator and guaranteed to be mycoplasma-free.

4.2.3. Screening assay to identify NOD1/2 dual inhibitors

HEK-Blue hNOD1 cells were seeded in 96-well plates at

50,000 cells/well, preincubated with compounds (10 μM) for 3 h, and stimulated with 50 ng/mL (~EC80) C12-iE-DAP (InvivoGen, San, Diego, CA) for 20 h. As we previously described [21], HEK-Blue hNOD2 cells were pretreated with different compounds (10 μM) for 3 h and then stimulated with 100 ng/mL (~EC_{80}) MDP (InvivoGen) for an additional 20 h. SEAP was detected using HEK-Blue detection (InvivoGen) and measured by a spectrophotometer at 655 nm according to the manufacturer's instructions. The inhibition rate (%) was determined using the following formula: inhibition (%) = {[C12-iE-DAP (OD655) or MDP (OD655) − compounds (OD655)]/[C12-iE-DAP (OD655) or MDP (OD655)]} × 100. Once the inhibition rate (%) was >50%, compounds were retested, and the SRB assay was conducted to exclude cytotoxicity. The IC_{50} values were determined using the GraphPad Prism 7 software [21].

4.2.4. In vitro metabolism and stability study

In stability studies using mouse liver microsomes, the incubation mixture contained phosphate buffer (100 mM, pH 7.4), liver microsomal protein (1.25 mg/mL) and compound (1.25 μM) in a total volume of 20 μL. After pre-incubation at 37 °C for 5 min, the reaction was initiated by adding an NADPH generating system [NADP (1 mM), $MgCl_2$ (10 mM), glucose 6-phosphate (10 mM), glucose-6-phosphate dehydrogenase (0.5 U/mL)]. The samples were then collected at 0, 5, 15, 30, 60 and 120 min after incubation, and the reaction was terminated by adding 300 μL Methanol/ACN (1:1, v/v). The mixtures were then centrifuged, and the supernatants were tested by LC−MS/MS assay. These assays were performed by BioDuro Technology Co., Ltd. (Shanghai, China).

4.2.5. Quantitative real-time PCR

The expression of mRNA was determined by quantitative reverse transcriptase-PCR analysis as previously described [21] and normalized to GAPDH. The following probes from Applied Biosystems were used for PCR analysis: human IL-6 (Hs00985639_m1), human IL-8 (Hs00174103_m1), human TNF-α(Hs01113624_g1), human GAPDH (Hs02758991_g1).

4.2.6. Western blotting

Cells were lysed in cold whole cell lysis buffer and the protein expression levels were determined as previously described [21]. Antibodies phosphor-IKKα/β (Ser176/180) (16A6) (no. 2697S), IKKα (no. 2682S), IKKβ (L570) (no. 2678S), phosphor-p65 (Ser536) (no. 3033), phosphor-p38 (no. 4631), p38 (no. 9212S), phosphor-JNK (no. CST9251S), JNK (no. 9252S), phosphor-RIP2 (no. 14397S), RIP2 (no. 4142) and IκBα (no. 9242S) were obtained from Cell Signaling Technology (Danvers, USA). Phosphor-ERK1/2 (sc-7383) and ERK1/2 (sc-94) antibodies were purchased from Santa Cruz Biotechnology (Santa Cruz, CA). Anti−NF−κB p65 (ab16502), anti-beta Actin antibody (HRP) (ab49900), goat polyclonal secondary antibody to rabbit IgG-H&L-HRP (ab6721) and rabbit polyclonal secondary antibody to mouse IgG-H&L-HRP (ab6728) were from Abcam (Cambridge, UK). The protein bands were developed by chemiluminescence (Thermo Scientific, Rockford, USA) with ChemiDoc XRS+ (Bio-Rad).

4.2.7. Animal experiment

C57BL/6 mice were kept in the animal research center laboratory of Tsinghua University for 1 week to adapt the environment. Each mouse was subcutaneously injected with B16F10 melanoma cells (2×10^5/0.1 mL in PBS) on the shoulder and left hind limb towards skeletal muscle. One day after implantation of cells, mice were divided into 4 groups randomly (n = 7 for each group): control vehicle, PTX, **36b**, PTX combined with **36b**. Mice were received intravenous injections with control vehicle or **36b** (50 mg/kg) every other day while PTX (12 mg/kg) every 4 days. PTX and **36b** were formulated in DMSO/Cremophor EL/saline at 5:5:90 (v:v:v). 11 days after implantation, primary tumor growths were measured using vernier calipers to determine the two orthogonal axes. The tumor volumes were calculated by formula (1/2) a^2b, where a is the shorter axis and b is the longer axis. 16 days after implantation, all mice were sacrificed. The primary tumors were removed, weighed, and photographed. Tumor weight inhibition was calculated by the following formula: [(C−T)/C] × 100 (C, tumor weight of vehicle group; T, tumor weight of treated group).

4.2.8. Statistical analysis

Statistical analyses were performed by two tailed Student's *t*-test, *P* values are indicated in the figure with statistically significant ($P < 0.05$). All results were confirmed in at least three independent experiments. All quantitative data were statistical analyzed with GraphPad software7.0.

Declaration of competing interest

The authors declare that they have no known competing financial interests or personal relationships that could have appeared to influence the work reported in this paper.

Acknowledgments

We gratefully acknowledge the funding support of grants from the National Natural Science Foundation of China (Grants 81803358, 81703329, 81273364 and 81773114) and Non-profit Central Research Institute Fund of Chinese Academy of Medical Sciences (2019-RC-HL-008).

Appendix A. Supplementary data

Supplementary data to this article can be found online at https://doi.org/10.1016/j.ejmech.2020.112723.

Abbreviations

Ac	acetyl group
AcOEt	acetic ether
BMDMs	bone marrow derived macrophages
Bz	benzoyl
BZD	1, 4-benzodiazepine-2, 5(H)-dione
C12-ie-DAP	lauroyl-γ-D-glutamyl-*meso*-diaminopimelic acid
CARD	caspase activation and recruitment domain
Calcd	calculated
CTX	cyclophosphamide
d	doublet
DAMPs	damage/danger-associated molecular patterns
DCM	dichloromethane
DIC	*N*,*N*′-Diisopropylcarbodiimide
DMAP	4-dimethylaminopyridine
DMF	*N*, *N*′-dimethylformamide
DMSO	dimethyl sulfoxide
DTX	docetaxel
eq	equivalent
ESI-MS	electrospray ionization-mass spectrometry
EtOAc	ethyl acetate
EtOH	ethanol
Glu	glutamic acid
Gly	glycine
HOAc	acetic acid
HOSu	N-hydroxysuccinimide
HPLC	high performance liquid chromatography
HR-MS	high resolution-mass spectrometry

Hz	hertz
IC50	50% inhibitory concentration
IBD	inflammatory bowel disease
IKK	inhibitor of nuclear factor kappa-B kinase
LC-MS	liquid chromatography-mass spectrometry
IL-6	interleukin-6
IND	investigational new drug
LRRs	leucine-rich repeats
m	multiplet;
m.p.	melting point
MAPKs	mitogen-associated protein kinases
MDP	N-acrtyl-MDP
MDSCs	myeloid-derived suppressor cells
MeOH	methanol
NACHT	nucleotide-binding domain
NF-κB	transcription factor nuclear factor κB
NMR	nuclear magnetic resonance
NOD	nucleotide-binding oligomerization domain
PAMPs	pathogen-associated molecular patterns
PTX	paclitaxel
q	quartet
RIP2	receptor-interacting sering/threonine-protein kinase 2
SAR	structure-activity relations
SEAP	secreted embryonic alkaline phosphatase
SRB	Sulforhodamine B
t	triplet
TEA	triethylamine
THF	tetrahydrofuran
TME	tumor microenvironment
TOF	time-of-flight
TNF-α	tumor necrosis factor-α.

References

[1] D.N. Khalil, E.L. Smith, R.J. Brentjens, J.D. Wolchok, The future of cancer treatment: immunomodulation, CARs and combination immunotherapy, Nat. Rev. Clin. Oncol. 13 (2016) 273–290.

[2] J.H. Fritz, R.L. Ferrero, D.J. Philpott, S.E. Girardin, Nod-like proteins in immunity, inflammation and disease, Nat. Immunol. 7 (2006) 1250–1257.

[3] R. Caruso, N. Warner, N. Inohara, G. Núñez, NOD1 and NOD2: signaling, host defense, and inflammatory disease, Immunity 41 (2014) 898–908.

[4] R.G. Correa, S. Milutinovic, J.C. Reed, Roles of NOD1 (NLRC1) and NOD2 (NLRC2) in innate immunity and inflammatory diseases, Biosci. Rep. 32 (2012) 597–608.

[5] C. Miceli-Richard, S. Lesage, M. Rybojad, A.-M. Prieur, S. Manouvrier-Hanu, R. Häfner, M. Chamaillard, H. Zouali, G. Thomas, J.-P. Hugot, CARD15 mutations in Blau syndrome, Nat. Genet. 29 (2001) 19–20.

[6] Y. Ogura, D.K. Bonen, N. Inohara, D.L. Nicolae, F.F. Chen, R. Ramos, H. Britton, T. Moran, R. Karaliuskas, R.H. Duerr, A frameshift mutation in NOD2 associated with susceptibility to Crohn's disease, Nature 411 (2001) 603–606.

[7] M. Saxena, G. Yeretssian, NOD-like receptors: master regulators of inflammation and cancer, Front. Immunol. 5 (2014) 327.

[8] L. Kager, U. Pötschger, S. Bielack, Review of mifamurtide in the treatment of patients with osteosarcoma, Therapeut. Clin. Risk Manag. 6 (2010) 279–286.

[9] S. Nabergoj, I. Mlinarič-Raščan, Ž. Jakopin, Harnessing the untapped potential of nucleotide-binding oligomerization domain ligands for cancer immunotherapy, Med. Res. Rev. 39 (2019) 1447–1484.

[10] R. Daillère, M. Vétizou, N. Waldschmitt, T. Yamazaki, C. Isnard, V. Poirier-Colame, Connie P.M. Duong, C. Flament, P. Lepage, Maria P. Roberti, B. Routy, N. Jacquelot, L. Apetoh, S. Becharef, S. Rusakiewicz, P. Langella, H. Sokol, G. Kroemer, D. Enot, A. Roux, A. Eggermont, E. Tartour, L. Johannes, P.-L. Woerther, E. Chachaty, J.-C. Soria, E. Golden, S. Formenti, M. Plebanski, M. Madondo, P. Rosenstiel, D. Raoult, V. Cattoir, Ivo G. Boneca, M. Chamaillard, L. Zitvogel, Enterococcus hirae and Barnesiella intestinihominis facilitate cyclophosphamide-induced therapeutic immunomodulatory effects, Immunity 45 (2016) 931–943.

[11] H.Y. Jiang, S. Najmeh, G. Martel, E. MacFadden-Murphy, R. Farias, P. Savage, A. Leone, L. Roussel, J. Cools-Lartigue, S. Gowing, J. Berube, B. Giannias, F. Bourdeau, C.H.F. Chan, J.D. Spicer, R. McClure, M. Park, S. Rousseau, L.E. Ferri, Activation of the pattern recognition receptor NOD1 augments colon cancer metastasis, Protein Cell 11 (2020) 187–201.

[12] Y. Dong, S. Wang, C. Wang, Z. Li, Y. Ma, G. Liu, Antagonizing NOD2 signaling with conjugates of paclitaxel and muramyl dipeptide derivatives sensitizes paclitaxel therapy and significantly prevents tumor metastasis, J. Med. Chem. 60 (2017) 1219–1224.

[13] Y. Ma, N. Zhao, G. Liu, Conjugate (MTC-220) of muramyl dipeptide analogue and paclitaxel prevents both tumor growth and metastasis in mice, J. Med. Chem. 54 (2011) 2767–2777.

[14] X. Wen, P. Zheng, Y. Ma, Y. Ou, W. Huang, S. Li, S. Liu, X. Zhang, Z. Wang, Q. Zhang, W. Cheng, R. Lin, H. Li, Y. Cai, C. Hu, N. Wu, L. Wan, T. Pan, J. Rao, X. Bei, W. Wu, J. Jin, J. Yan, G. Liu, Salutaxel, a conjugate of docetaxel and a muramyl dipeptide (MDP) analogue, acts as multifunctional prodrug that inhibits tumor growth and metastasis, J. Med. Chem. 61 (2018) 1519–1540.

[15] D.J. Rickard, C.A. Sehon, V. Kasparcova, L.A. Kallal, P.A. Haile, X. Zeng, M.N. Montoute, D.D. Poore, H. Li, Z. Wu, P.M. Eidam, J.G. Emery, R.W. Marquis, P.J. Gough, J. Bertin, Identification of selective small molecule inhibitors of the nucleotide-binding oligomerization domain 1 (NOD1) signaling pathway, PloS One 9 (2014), e96737.

[16] P.M. Khan, R.G. Correa, D.B. Divlianska, S. Peddibhotla, E.H. Sessions, G. Magnuson, B. Brown, E. Suyama, H. Yuan, A. Mangravita-Novo, M. Vicchiarelli, Y. Su, S. Vasile, L.H. Smith, P.W. Diaz, J.C. Reed, G.P. Roth, Identification of inhibitors of NOD1-induced nuclear factor-κB activation, ACS Med. Chem. Lett. 2 (2011) 780–785.

[17] Ž. Jakopin, Nucleotide-binding oligomerization domain (NOD) inhibitors: a rational approach toward inhibition of NOD signaling pathway, J. Med. Chem. 57 (2014) 6897–6918.

[18] D.J. Rickard, C.A. Sehon, V. Kasparcova, L.A. Kallal, X. Zeng, M.N. Montoute, T. Chordia, D.D. Poore, H. Li, Z. Wu, P.M. Eidam, P.A. Haile, J. Yu, J.G. Emery, R.W. Marquis, P.J. Gough, J. Bertin, Identification of benzimidazole diamides as selective inhibitors of the nucleotide-binding oligomerization domain 2 (NOD2) signaling pathway, PloS One 8 (2013), e69619.

[19] Ž. Jakopin, E. Corsini, THP-1 cells and pro-inflammatory cytokine production: an in vitro tool for functional characterization of NOD1/NOD2 antagonists, Int. J. Mol. Sci. 20 (2019) 4265.

[20] K.K. Plešec, D. Urbančič, M. Gobec, A. Pekošak, T. Tomašič, M. Anderluh, I. Mlinarič-Raščan, Ž. Jakopin, Identification of indole scaffold-based dual inhibitors of NOD1 and NOD2, Bioorg, Med. Chem. 24 (2016) 5221–5234.

[21] S. Wang, J. Yang, X. Li, Z. Liu, Y. Wu, G. Si, Y. Tao, N. Zhao, X. Hu, Y. Ma, G. Liu, Discovery of 1, 4-benzodiazepine-2, 5-dione (BZD) derivatives as dual nucleotide binding oligomerization domain containing 1/2 (NOD1/NOD2) antagonists sensitizing paclitaxel (PTX) to suppress Lewis lung carcinoma (LLC) growth in vivo, J. Med. Chem. 60 (2017) 5162–5192.

[22] J. Yang, X. Hu, Z. Liu, X. Li, Y. Dong, G. Liu, Cp*Co-III-catalyzed formal 4+2 cycloaddition of benzamides to afford quinazolinone derivatives, Chem. Commun. 55 (2019) 13840–13843.

[23] A. Larsen, P.M. Lish, A new bio-isostere: alkylsulphonamidophenethanolamines, Nature 203 (1964) 1283–1284.

[24] S. Roderick, M. Fournie-Zaluski, B. Roques, B. Matthews, Thiorphan and retrothiorphan display equivalent interactions when bound to crystalline thermolysin, Biochemistry 28 (1989) 1493–1497.